Karakterizacija novonastalog tkiva nakon biopsije hrskavice nosne pregrade

Brezak, Matea

University of Zagreb

Faculty of Science

Department of Biology

Matea Brezak

CHARACTERIZATION OF NEWLY-FORMED TISSUE AFTER NASAL SEPTUM CARTILAGE BIOPSY

Graduation Thesis

Zagreb, 2019

This thesis was made in the Laboratory of Biomedicine at Division of Molecular Biology, Faculty of Science, under the supervision of Dr Inga Marijanović, Assoc. Prof. and research assistant Maja Pušić, mag. biol. exp.
The thesis was submitted for evaluation to the Department of Biology, Faculty of Science in order to acquire title the Master of molecular biology.

BASIC DOCUMENTATION CARD

University of Zagreb

Faculty of Science

Department of Biology

Graduation Thesis

CHARACTERIZATION OF NEWLY-FORMED TISSUE AFTER NASAL SEPTUM CARTILAGE BIOPSY

Matea Brezak

Rooseveltov trg 6, 10000 Zagreb, Croatia

Tissue engineering has become one of the most studied fields with clinical application. When producing cartilage tissue *in vitro*, nasal septum biopsy is taken in order to harvest chondrocytes that will be seeded on scaffolds. Following this procedure, the nasal septum is left with a perforation that fills in over time. The newly-formed tissue may not possess functional properties characteristic for septum cartilage, whereas if the neocartilage forms it would enable chondrocyte reharvesting and confirm normal septum function. To this time, no one has addressed the issue of tissue formation in the place of the perforation on a large animal model. Therefore, in this study, newly-formed tissue was characterized using histological and immunohistochemical stainings including analysis of cartilage and perichondrium marker gene expression. Low regenerative potential of cartilage was confirmed as no formation of similar tissue was observed over time. Perichondral origin of newly-formed tissue was confirmed both histologically and through gene expression analysis. Additionally, high expression of COL 1, COL 4 and CRABP 1 genes indicate a significant role of outer perichondrium layer in tissue genesis.

(29 pages, 11 figures, 9 tables, 46 references, original in: English)
Thesis deposited in the Central Biological Library.
Keywords: gene expression, immunohistochemical analysis, nasal cartilage, perichondrium, tissue engineering
Supervisor: Dr Inga Marijanović, Assoc. Prof.
Assistant Supervisor: Maja Pušić, mag. biol. exp.
Reviewers:
Dr Inga Marijanović, Assoc. Prof.
Dr Romana Gračan, Assis. Prof.
Dr Nada Oršolić, Prof.
Thesis accepted: 31.2.2019

TEMELJNA DOKUMENTACIJSKA KARTICA

Sveučilište u Zagrebu

Prirodoslovno-matematički fakultet

Biološki odsjek Diplomski rad

KARAKTERIZACIJA NOVONASTALOG TKIVA NAKON BIOPSIJE HRSKAVICE NOSNE PREGRADE

Matea Brezak

Rooseveltov trg 6, 10000 Zagreb, Hrvatska

Danas se u liječenju oštećenja zglobne hrskavice ili hrskavice nosne pregrade sve češće koriste tkivni presatci dobiveni metodama tkivnog inženjerstva. Prilikom uzgoja tkivnih presadaka potreban je izvor stanica koje će se nasaditi na nosač, te se u tu svrhu uzima biopsija hrskavice nosne pregrade. Uslijed tog postupka, na mjestu biopsije ostaje praznina koja se tijekom vremena ispuni tkivom nepoznatog porijekla i morfologije. Do sada nisu provedena istraživanja na velikim modelnim organizmima koja bi dokazala posjeduje li novonastalo tkivo svojstva potrebna svojstva da bi se održala normalna funkcija pregrade. Ukoliko se formira novo hrskavično tkivo funkcionalnost ne bi bila ugrožena te bi se omogućilo ponovno uzimanje hondrocita s istoga mjesta. Cilj ovog istraživanja je putem histoloških i imunohistokemijskih bojanja, kao i analizom ekspresije gena metodom qPCR okarakterizirati novonastalo tkivo na mjestu biopsije. Histološka analiza je pokazalaniski regenerativni potencijal hrskavičnog tkiva kao i ulogu perihondrija u stvaranju novog tkiva. Analiza ekspresije gena novonastalog tkiva je potvrdila histološke rezultate.. Dodatno, visoka ekspresija gena COL 1, COL 4 i CRABP 1 potvrdila je značajnu ulogu vanjskog fibroznog sloja perihondrija u nastanku novog tkiva.

(29 stranica, 11 slika, 9 tablica, 46 literaturna navoda, jezik izvornika: engleski)
Rad je pohranjen u Središnjoj biološkoj knjižnici.
Ključne riječi: ekspresija gena, hrskavica nosnog septuma, imunohistokemijska analiza, perihondrij, tkivno inženjerstvo
Voditelj: Dr. sc. Inga Marijanović, izv. prof.
Neposredni voditelj: Maja Pušić, mag. biol. exp.
Ocjenitelji:
Dr. sc. Inga Marijanović, izv. prof.
Dr. sc. Romana Gračan, doc.
Dr. sc. Nada Oršolić, prof.
Rad prihvaćen: 31.2.2019.

Table of Contents

Abbreviations:

AGG - aggrecan

cDNA - complementary DNA

COL 1 - collagen type I

COL 2 - collagen type II

COL 4 - collagen type IV

COMP - cartilage oligomeric matrix protein

CRABP 1 - Cellular Retinoic Acid Binding Protein-I

CV - critical value

DAB - 3, 3 -diaminobenzidine

DEPC - diethyl pyrocarbonate

DF - degree of freedom

DKK 3 - Dickkopf WNT Signaling Pathway Inhibitor 3

DNA - deoxyribonucleic acid

ECM - extracellular matrix

EDTA - ethylenediaminetetraacetic acid

FC - fold change

GAG - glycosaminoglycan

GAPDH - glyceraldehyde 3-phosphate dehydrogenase

H&E - hematoxylin-eosin

MSC - mesenchymal stem cells

NFT - newly-formed tissue

PBS - phosphate-buffered saline

PCR - polymerase chain reaction

qRT-PCR - quantitative real-time polymerase chain reaction

RNA - ribonucleic acid

RT - room temperature

TAE - Tris-acetate-EDTA

TERM - tissue engineering and regenerative medicine

1. INTRODUCTION

Tissues are organized aggregations of cells that perform some specific functions. Regardless of variations in appearance, organization and physiological properties, the tissues that compose body organs are classified into four types. Epithelial, connective, muscle and nerve tissue are defined by a specific set of morphologic and functional characteristics. The cells of epithelial tissue are always tightly bound together what enables this tissue to cover body surfaces and cavities. The most prominent characteristic of muscle tissue is the ability of its cells to contract, therefore resulting in movement. The nerve tissue contains nerve cells and various supporting cell types, but its main purpose is to receive, transmit and integrate information in order to control every process in the body. Finally, the connective tissue consists of many cell types and is characterised through extracellular matrix composition. Due to that, connective tissue is generally subclassified into loose or dense and specialised forms (Pollard et al. 2017).

1.1. Connective tissue

The basic function of connective tissue is to fill spaces between organs and other tissues while providing structural and metabolic support. In general, it consists of cells and extracellular matrix (ECM). The cells are embedded in the matrix made of glycoproteins, fibrous proteins and glycosaminoglycans. Different cell types produce and secrete various ECM components hence giving specific properties to the connective tissue subtype. Based on the function, composition and organization of cellular and extracellular components connective tissue is subclassified into loose and dense connective tissue, with later being divided into regular and irregular. Except for the above, specialized connective tissue makes another type of connective tissue which is further divided into adipose tissue, cartilage, blood, bone, hemopoietic and lymphatic tissue (Table 1.; Ross and Pawlina 2010).

Table 1. Connective tissue subclasses with main morphological and functional properties

CONNECTIVE TISSUE	CHARACTERISICS	FUNCTION
CONNECTIVE TISSUE PROPER		
LOOSE CONNECTIVE TISSUE	• loosely arranged fibres and cells of various types	• diffusion • inflammatory and immune reactions
DENSE IRREGULAR CONNECTIVE TISSUE	• few cells and abundant fibres oriented in various directions	• structural support • resistance to tearing and stretching
DENSE REGULAR CONNECTIVE TISSUE	• parallely oriented and densely packed fibres with cells aligned between them	• resistance to tension forces while allowing some stretch
SPECIALIZED CONNECTIVE TISSUE		
ADIPOSE TISSUE	• loose connective tissue with the most frequent cell type being adipocytes	• storage of energy in form of triglycerides • energy metabolism regulation
CARTILAGE	• chondrocytes embedded in specialized ECM made up of water, fibres (mostly collagens), proteoglycans and glycoproteins	• template for growth and development of long bones • structural support • formation of articulating surfaces for bones

BLOOD	• fluid connective tissue that contains cells (erythrocytes, leukocytes and thrombocytes) in liquid ECM called plasma	• transport of cells, hormones, nutrients and wastes • homeostasis maintenance
BONE	• mineralized ECM with lacunae containing osteocytes • associated cells: osteoblasts, osteoclasts and osteoprogenitors	• support and protection of soft tissues • calcium and phosphate storage (homeostasis regulation)
HEMOPOIETIC TISSUE	• tissue containing hemopoietic stem cells (bone marrow)	• blood cell production
LYMPHATIC TISSUE	• diffuse lymphatic tissue (MALT) that is not enclosed by a capsule • lymphatic nodules which are aggregations of lymphocytes and reticular cells	• proliferation, differentiation and maturation of lymphocytes

1.2. Cartilage

Cartilage is a connective tissue composed of cells called chondroblasts and chondrocytes that secrete extensive extracellular matrix. As the chondroblasts secrete ECM components they become trapped inside it and mature into chondrocytes. As they continue to secrete matrix components, they surround themselves forming enclosed compartments called lacunae. During this process, chondrocytes can divide thereby, developing clusters of 2-4 cells called isogenous groups. As newly-formed chondrocytes in isogenous groups continue to produce the matrix components they are being separated and form individual lacunae. At this time, chondrocytes also secrete metalloproteinases that enable matrix degradation and chondrocyte reposition within the cartilage matrix. Due to such organization, cartilage has up to 5% cellular content with the rest being extracellular matrix made up of fibres and ground substance (Ross and Pawlina 2010).

Since cartilage is an avascular tissue it is crucial for the matrix to have properties that enable diffusion of nutrients and signals needed for the chondrocyte homeostasis. Such properties are achieved through the matrix components that attract water and create the pores of different sizes. Main constituents of ECM are collagen fibres, an amorphous ground substance composed of glycosaminoglycans (GAGs), and multiadhesive glycoproteins. Glycoproteins mediate the chondrocyte and matrix molecules interactions. A complex collagen network is laid in ground substance where it entraps proteoglycan aggregations and provides tensile resistance to the tissue. Glycosaminoglycans bind to a core protein, therefore, creating negatively charged proteoglycans that attract water molecules. High water content with aggregates of proteoglycans makes cartilage prone to compressive forces and serve as a perfect medium for molecular diffusion (Grassel and Aszodi 2016).

As a result of subtle differences in ECM composition, three types of cartilage emerge; hyaline, elastic and fibrocartilage. Hyaline cartilage is the most common and is found in ribs, nose, larynx, trachea and as a part of articular surfaces. The collagen component of hyaline cartilage mostly consists of type II collagen fibres whereas the aggrecan is the most prominent proteoglycan monomer in the ground substance. Within the elastic cartilage, except for the components of hyaline cartilage, lies a dense meshwork of elastic fibres. These additional constituents give the cartilage elastic properties that correspond to the function and location of this tissue in the external ear and epiglottis. Finally, fibrocartilage as the strongest cartilage type is present in intervertebral discs, menisci, symphysis pubis and at the sites of tendons attaching to the bone. Along with chondrocytes it contains fibroblasts and has alternating layers of hyaline cartilage and dense regular connective tissue. Another significant difference is in matrix composition as the fibrocartilage contains equal quantities of both collagen type II and I, as well as higher amounts of proteoglycan versican (Ross and Pawlina 2010).

1.3. Hyaline cartilage

As mentioned before, hyaline cartilage is the most frequent type of cartilage and one of its main functions is to provide low-friction surface and participate in the movement. Owing to that, the most studied type of cartilage is articular hyaline cartilage which is surrounded by synovial fluid. Hyaline cartilage in head and neck region is, in contrary, surrounded by a layer of dense connective tissue named perichondrium. In general, hyaline cartilage consists of 60–80% of the wet weight of intercellular water, about 15% collagen molecules, 10% ground substance components and only of 3–5% cells. Those 3–5% of chondrocytes produce and secrete components of hyaline cartilage extracellular matrix (Ross and Pawlina 2010). Major groups of ECM components are collagen molecules, proteoglycans and multiadhesive glycoproteins.

The cartilage extracellular matrix is a fibre-reinforced gel produced by a surprisingly low number of cells. Chondrocytes are highly specialized cells situated in cartilage ECM either singularly or in isogenous groups (Figure 1.). Variations in shape, number and size of chondrocytes are evident mainly throughout the articular cartilage but also in hyaline cartilage in other anatomical sites (Fox, Bedi, and Rodeo 2009). During development, they arise either from the mesodermal origin or from the neural crest, but as the growth ceases they loose ability of division (Archer and Francis-West 2003). Never the less, chondrocytes continue to fulfil their primary function of producing and sustaining the extracellular matrix for as long as the organism lives, therefore, being considered long-living cells. Also, they participate in the internal remodelling of cartilage by compensating matrix components lost due to degradation. During the organism development, chondroblasts and chondrocytes contribute to cartilage growth by the means of appositional or interstitial growth (Muir 1995). As fully developed cartilage is hypocellular, aneural, alymphatic and avascular tissue, its nutrition depends solely on diffusion and due to that, chondrocytes have to be well adapted to low oxygen conditions. To withstand such an environment, chondrocytes use anaerobic metabolism and glycolysis which provide energy for survival and synthesis of ECM components (Mobasheri et al. 2018).

The most abundant structural components of ECM are collagen fibres with the type II collagen representing 90 – 95% of all ECM collagens. Its prime role is to form fibrils and fibres that will interact with proteoglycan aggregates. Collagen types I, IV, V, VI, IX and XI represented in smaller proportions, contribute to the formation and stabilization of type II collagen meshwork. All collagen family members consist of three polypeptide chains that coil around one another and form a triple helix structure. Each of polypeptide chains contains a triple helix domain with Gly-X-Y repeats, with X most often being proline, and Y being hydroxyproline amino acid (Cooper and Hausman 2016). Collagen type II consists of three identical polypeptide chains marked as α1 chains. Each of them is distinct gene product differing in primary structure from the other α chains that constitute other collagen types. Due to its wide presence in hyaline cartilages and absence from most of the other tissues, type II collagen is considered to be cartilage-characteristic (Ali et al. 1983).

Another major structural component of ECM are proteoglycans, heavily glycosylated protein monomers. Each protein core has one or more linear glycosaminoglycan chains covalently attached to it. Chains consist of repeating disaccharides, mainly N-acetylglucosamine or N-acetylgalactosamine, and can contain up to 100 sugar residues. More than 100 GAGs can be linked to a core protein, all extending from the core protein and remaining separated from each other due to charge repulsion (Fox et al. 2009). Sugars that form GAGs are modified by the addition of sulfate groups and consequently, become highly negatively charged. From that surfaces its main purpose to entrap water molecules and form a hydrated gel that will serve as the ground substance of ECM. The most common sulfated GAGs found in hyaline cartilage are chondroitin sulfate and keratan sulfate. Hyaluronan does not contain sulfate groups and is the only GAG that persists as a single polysaccharide chain. Hyaline cartilage contains a variety of proteoglycans including aggrecan, decorin, biglycan and others. The most abundant, and the largest in size is aggrecan known for its ability to interact with hyaluronan through the aid of link proteins and to form tremendous aggregates (Figure 1A.) (Cooper and Hausman 2016). Exactly this aggregates provide

cartilage with the critical properties for its role and function in the organism, as entrapped water changes osmotic properties of the tissue. Other proteoglycans are much smaller than aggrecan but are represented in similar quantities as they are crucial for interactions between other ECM components (Fox et al. 2009). For example, decorin has an important role in collagen fibrillogenesis as it helps to orient the fibres and regulates the fibril thickness.

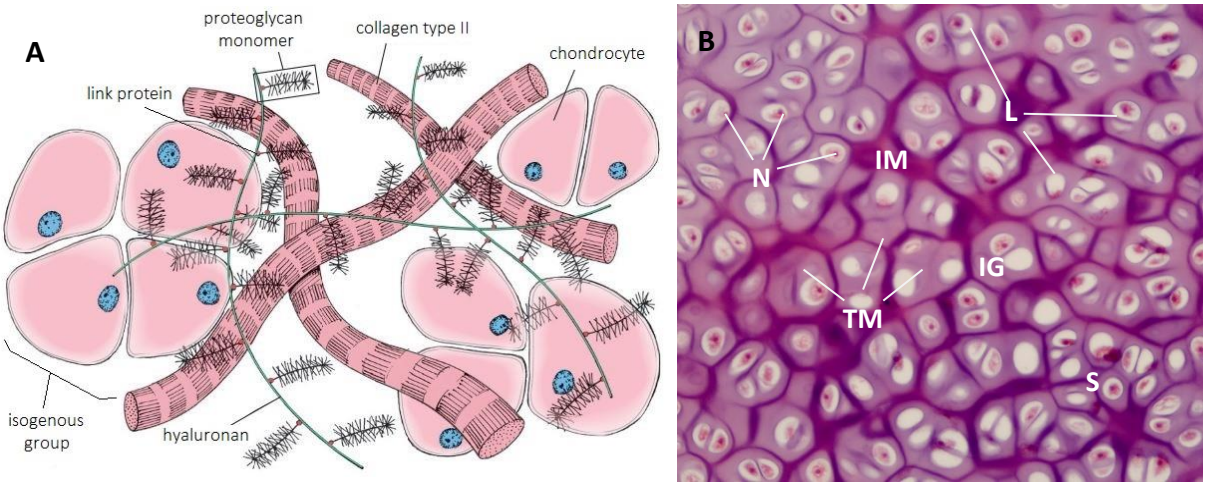

Figure 1. A) Schematic diagram of the hyaline cartilage matrix molecular structure. Chondrocytes secrete ECM components and become embedded in the matrix. The proteoglycan monomers, constituted from glycosaminoglycans bound to the core protein, are connected to a hyaluronan molecule by a link protein. Collagen type II fibres form a complex network that entraps large negatively charged proteoglycan aggregates whose role is to attract and bind water molecules (modified according to Ross & Pawlina 2010). **B) Nasal septum hyaline cartilage specimen stained in H&E, 10x magnification**. Mature chondrocytes with visible nuclei are entrapped in ECM and residue in lacunae singularly or in isogenous groups. They produce the cartilage matrix that shows darker or interterritorial and lighter or territorial matrix. N – nuclei; L – lacunae; S – singular chondrocyte; IG – isogenous group; IM – interterritorial matrix; TM – territorial matrix

Finally, multiadhesive glycoproteins are the third major class of ECM molecules. They participate in interactions between the chondrocytes and the matrix molecules, therefore, stabilizing the ECM. The variety of binding sites for ECM components such as collagens, proteoglycans and GAGs, as well as for the cell-surface receptors allow these proteins to regulate and modulate functions of ECM. Some of the most studied multiadhesive glycoproteins are anchorin CII, tenascin, perlecan and fibronectin. All of them are found in many tissues other than cartilage as they have an almost universal role in cell and ECM interactions (Ross and Pawlina 2010). Cartilage oligomeric matrix protein (COMP) is another characteristic representative of this group. It is expressed primarily in cartilage where it functions as a regulator of chondrocyte proliferation, collagen type II fibrils polymerization and mediates ECM-cell interactions. Besides these interactions, it has been recently shown that COMP binds many transcription and growth factors, therefore, regulating cartilage homeostasis. Also, it has an active role in inflammation by simultaneously activating and inhibiting complementary pathways (Zaucke 2016).

1.4. Perichondrium

In the cartilage template area of a growing bone, during development and growth, as well as in the head and neck region, hyaline cartilage is covered with firmly attached tissue called perichondrium. This regular dense connective tissue is the last area to which nerves, blood and lymphatic vessels protrude. Due to its fibrous, but porous nature it facilitates the provision of oxygen and necessary nutrients to the cartilage. It is composed of fibroblast-like cells and few layers of connective tissue fibres parallel to the cartilage (Ross and Pawlina 2010). During growth, it also represents the source of new

cartilage cells and can be divided into an outer fibrous layer, and an inner cellular (cambium) layer. The inner layer contains fibroblast-like cells and cartilage progenitors, wherefore, it contributes to new cartilage cell production and tissue growth. On the contrary, outer fibrillar layer, mostly containing collagen type I fibres (Bleys et al. 2007) and fibroblasts, provides mechanical support and protection while connecting cartilage to surrounding tissue (Aksoy et al. 2012).

As a response to injury of cartilage and perichondrium, the inner cambium layer begins to produce new cells in the wound healing process, wherefore it is considered to harbour progenitor cells and serve as a mesenchymal stem cell (MSC) reservoir (Skoog, Ohlséan, and Sohn 1972). In their research, Kaiser et al. (2006), have shown that preserved perichondrium, as a mesenchymal stem cell source, actively contributes to the formation of neocartilage in a place of the induced lesion. The proliferation rate of MSC and progenitor cells in the inner cambium layer is lower than the proliferation rate of fibroblast cells in the outer fibrous layer. As a result, when both cartilage and perichondrium are injured, fibrous layer outgrows the edges of cartilage what leads to the formation of non-cartilaginous tissue (Duynstee et al. 2002).

Recently, many efforts have been made to uncover the molecular markers of the perichondrium. Collagen type II (COL2A1), aggrecan (AGG) and cartilage oligomeric matrix protein (COMP) are widely used as markers for hyaline cartilage tissue and can be used as perichondrium excluding markers. At the moment, the most widely used perichondrium marker is collagen type I. Although, hyaline cartilage does not contain collagen type I molecules, it is broadly represented in all other connective tissues. Bone is one such tissue with approximately 95% collagen type I content (Farach-Carson, Eagner, and Kiick 2007). However, collagen type I is good perichondrium indicator, especially for immunohistochemical tissue analysis and, with certain precautions, can be used as a marker in other tissue characterization methods (Treilleux et al. 1992). With the development of high throughput methods, new foundings have come to focus. One such research elucidates potential perichondrium markers at the same time categorizing them into inner or outer layer markers. Thrombospondin 2 (Tsp 2), Galectin-1, Dickkopf WNT Signaling Pathway Inhibitor 3 (Dkk3), and transcription factor MafB are some of the transcripts localized to inner cambium layer of the perichondrium. In addition, increased expression of Undulin (COL14A1) and Cellular Retinoic Acid Binding Protein-I (CRABP-I) has been shown in outer fibrillar layer (Bandyopadhyay et al. 2008). Similar research has been conducted by Hinton et al. (2009) who highlighted collagen type IV and XIV as highly expressed in perichondrium comparing to the cartilage. Although these genes show higher expression throughout perichondrium and can be used as markers, neither of them is found specifically in perichondrium, therefore they are to be referred as perichondrium-characteristic.

1.5. Cartilage development and regeneration

Chondrogenesis is a dynamic cellular process which denotes the formation of cartilage. It involves recruitment and migration of mesenchymal stem cells (MSC), the formation of progenitor condensations, and chondrocyte differentiation. Growth and differentiation factors are one, but not a crucial factor in cartilage formation. Cellular interactions with the surrounding matrix, as well as other environmental factors, play important role in regulating specific signalling pathways that will lead to cartilage development. Three different embryonic cell populations contribute to cartilage formation. In most of the body, cartilage develops from paraxial mesoderm and lateral plate mesoderm, respectively. In the head region, the majority of cartilaginous elements originates from cranial neural crest cells.

Undifferentiated MSCs retract their cytoplasmic extensions, therefore, assuming a rounded shape. Consequently, they migrate and tightly pack to form dense aggregates at the centre of chondrification thus creating a mesenchymal precartilage condensation. At this point cells produce ECM rich in collagen type I, hyaluronan, and fibronectin (DeLise, Fischer, and Tuan 2000). Increase in cellular contacts triggers chondroblast differentiation as the specific signalling pathways are activated. Chondroblasts at the core of the condensation start secreting matrix components including, collagen type

II, IX, XI, aggrecan and link protein while consequently growing apart from each other. As the production of matrix continues, the COMP becomes abundant in ECM and chondroblasts transition into fully committed chondrocytes (Goldring, Tsuchimochi, and Ijiri 2006). Meanwhile, at the periphery of mesenchyme condensation cells receive signals that lead them to the formation of dense regular connective tissue termed perichondrium (DeLise et al. 2000).

As the tissue forms, the growth begins by two distinct processes. During interstitial growth, chondrocytes go through mitosis, therefore, forming isogenous groups. New chondrocytes secrete matrix components, as well as metalloproteinases, needed for matrix remodelling through which chondrocytes expand from the site of the isogenous group. The volume and mass of the cartilage increase as the new chondrocytes deposit matrix components and again entrap themselves during the process. Appositional growth, or growth at a tissue surface, involves stem cells in the inner layer of the perichondrium. As the centre of the growing cartilage becomes more rigid and contains only mature chondrocytes, the peripheral parts tend to house mesenchymal progenitor cells. These cells have the ability to become either components of perichondrium (mostly fibroblasts) or chondroblasts that will subsequently become chondrocytes. Due to different signalization, chondroblasts will secrete matrix components and contribute to cartilage growth at the periphery (Ross and Pawlina 2010).

Due to function and localization, cartilage is prone to injuries. When damaged, the ability to heal is insignificant, and the repair mostly involves the production of other connective tissue. The inability to heal is associated with the cartilage avascularity, chondrocyte immobility and limited proliferation rate. In articular cartilage, during the healing process, inflammatory cells enter the injured site, and matrix degradation begins following with deposition of matrix proteins by surrounding chondrocytes (Sharifi, Moshiri, and Oryan 2016). The healing often results in the formation of scar tissue mainly composed fo fibrocartilage. However, when the damage includes hyaline cartilage with belonging perichondrium some repair can occur. As noted before, perichondrium contains an outer and inner layer with distinct molecular characteristics. The inner layer contains cartilage progenitors that can produce both collagen type I and II fibres, meaning it can give rise to fibroblasts, found in perichondrium, and chondroblasts, found in cartilage. Several studies have shown new cartilage formation in both young and mature organisms when perichondrium is present in the place of injury (Kaiser et al. 2006); Duynstee et al. 2002). Kaiser et al. (2006) have noted few neocartilage islands in the place of cartilaginous nasal septum lesion, formed due to the activity of cells from inner perichondrium layer. Morphologically, neocartilage resembles native septal cartilage but is not identical and mechanical behaviour may not be the same.

1.6. Tissue engineering in cartilage regeneration research

Since cartilage has poor ability to heal and is prone to injuries that tend to become chronic conditions such as osteoarthritis, methods for treatment of such injuries are a continuous research subject. Various options have been used for the treatment of articular cartilage defects, including the conservative approach that encompasses physiotherapy and pharmacological agents, as well as surgical procedures. As many of these procedures do not offer long-term recovery and are mostly oriented towards symptom alleviation, TERM (tissue engineering and regenerative medicine) approach has come to light as a new and improved method for cartilage defects treatment. Except the pain relieve, TERM aims to temporary fill the defect while enhancing cartilage function, and to control and accelerate production of neocartilage with similar properties as native cartilage (Sharifi et al. 2016). The procedure involves either tissue scaffolds, cells or healing promotive factors that will aid in cartilage regeneration. Generally, autologous cells are isolated from a small biopsy, expanded *in vitro* and used to engineer implantable grafts. Although the procedure has been shown as successful, further studies aim to improve scaffolds, expansion and engineering procedures, as well as to find the best cell source for cartilage grafting. Through the years, several cell sources have come to focus (Table 2), among which chondrocytes form fully mature nasal septum cartilage have proved to be the most suitable.

Table 2. Cell sources for tissue-engineered cartilage with main advantages and disadvantages (modified according to Johnstone et al. 2012 and Liu et al. 2017)

CELL TYPE	ADVANTAGES	DISADVANTAGES
Nasal chondrocytes	• Native phenotype • Easy harvesting • Higher proliferation rate	• Small initial cell number • Dedifferentiation
Articular chondrocytes	• Native phenotype	• Difficult harvesting • Secondary injury induction • Small initial cell number • Dedifferentiation
Adult mesenchymal stem cells	• Various harvest sites • Potential to produce large numbers • Generation of bone and cartilage	• Several cell subpopulations • Potential for hypertrophy • Unstable chondrogenic phenotype
Induced pluripotent stem cells	• Production of multiple cell types	• Potential for teratoma • Problematic stable differentiation
Embryonic stem cells	• Production of multiple cell types	• Potential for teratoma • Problematic stable differentiation

Adult chondrocytes with the ability to form an ECM can be isolated from various sources such as articular cartilage, nasal septum, auricular of costal cartilage. As for the articular cartilage engineering hyaline cartilage is preferred, nasal septum chondrocytes have been shown as superior over other sources (Vinatier and Guicheux 2016). Articular chondrocytes can be used as a source for tissue grafting, but as harvesting involves biopsy in a non-weight bearing site the additional injury to the joint inflicted and can lead to future osteoarthritis development. In contrary, nasal septum biopsies are harvested under local anaesthesia and cause minimal donor site morbidity. Also, it has been shown that nasal chondrocytes have a higher proliferation rate, and are capable of retaining their capacity to generate hyaline-like tissue after the dedifferentiation, both *in vitro* and *in vivo* (Pelttari, Wixmerten, and Martin 2009). Farhadi et al. (2006) have shown that mechanical properties of cartilage grafts made with nasal chondrocytes are similar to those of native cartilage. Moreover, grafted tissue quality is not highly dependent on donor age and is histologically and mechanically superior to that generated from articular chondrocytes (Rotter et al. 2002). More recently, nasal chondrocyte engineered cartilage grafts were implanted in a place of the articular cartilage defect, where they displayed the ability to adapt to the recipient site. The organisation of regenerated tissue was highly similar to the native articular cartilage and the cells have adopted gene expression characteristic for the native tissue (Pelttari et al. 2014). All of these findings contribute to broader use of nasal septum chondrocytes as a cell source for cartilage grafting.

The prime goal of any cartilage repair research is to develop methods and treatments that will be successfully introduced to the clinic. Essential components in achieving this goal are translation animal models. Depending on the type of research different animals are used. Small animal models like rodents (mouse, rat and rabbit) are mostly used for studying basic action mechanisms and as a model prior to study on a large animal model. Large animals most commonly used in articular cartilage repair research are dogs, sheep, goats or horses (Chu, Szczodry, and Bruno 2010). Based on the focus of the research, either of the models can be exploited. Studies that have cartilage biomechanics in focus will benefit the most from the horse model, while those that study post-operative recovery will do best with a dog model as bandages and orthotics can be used. Translational pre-clinical studies that do not require specific post-operative management mostly use goat or sheep models (Cook et al. 2014). Although the cartilage thickness, joint size and movement of both goats and sheep most closely resemble human, sheep are more preferable as goats tend to climb fences what introduces the additional risk of self-inflicted injury (Music, Futrega, and Doran 2018). Mumme et al. (2016) have tested tissue-engineered grafts generated by nasal chondrocytes for the repair of articular cartilage in a large animal study and showed efficient

integration of this grafts in the surrounding tissue. Following this large animal study, two clinical trials have been carried out on a small number of patients to confirm previous findings (Mumme et al. 2016b). After a positive outcome, larger trials are conducted to fully introduce the new treatment to the clinic.

1.7. Aims of research

Avascularity, high ECM content and low cellularity limit cartilage ability to self-renew following the injury. Due to that, the tissue engineering approach has become more frequent and many studies aim to develop better cultivation methods, scaffolds and find better cell sources. Nasal septum chondrocytes have emerged as an optimal cell source for tissue grafting due to its proliferation rate, age independence and tissue plasticity. In order to obtain nasal septum chondrocytes, a biopsy is performed under local anaesthesia. This procedure leaves septum with a small perforation that fills in over time. The morbidity at the place of biopsy is minimal, but the newly-formed tissue may not have the same functional characteristics as the native cartilage. Therefore, the goal of this research is to examine and characterise the tissue formed in the place of the perforation on large animal model. If neocartilage forms it would enable re-explantation of chondrocytes from the same area as well as confirm the normal function of nasal septum after the procedure. When taking a biopsy from sheep nasal septum, perichondrium which is tightly bound to cartilage is damaged as well. Knowing the nature of perichondrium, the assumption is that the outer fibroblast layer will outgrow the edges of cartilage and inhibit the activity of the inner cambium layer and nearby chondrocytes. Therefore, it is expected for perforation to be filled out with dense, regular connective, perichondrium-like tissue. To confirm or refute these claims, explanted septum tissues are to be histologically stained and examined. To complement histological analysis, RNA will be isolated from both newly-formed and native tissue, whereupon it will be purified from any DNA residue and transcribed into cDNA that will be used for PCR and qRT-PCR analysis. The expression of specific cartilage and perichondrium marker genes will be determined by qRT-PCR to additionaly examine differences between newly-formed and native cartilage tissue.

2. MATERIALS AND METHODS

2.1. Experimental groups / Tissue harvest

Eighteen mature domestic sheep *Ovis aries aries* (Linnaeus, 1758.) aged 3 to 5 years underwent biopsy of the cartilaginous nasal septum with perichondrium layer (8 mm in diameter). Two or six months after, explantation of cartilaginous nasal septum part containing the place of the previous biopsy was performed. Sheep cartilaginous nasal septum explantations were carried out, with the approval of the Ethical Committee, at the University of Zagreb, Faculty of Veterinary Medicine in the Clinic for Surgery, Orthopedics, and Ophthalmology.

Following the explantation, samples were cut in half with one half taken for histological analysis and other for gene expression analysis through qRT-PCR. Except for the cartilage with perichondrium, mucosa and submucasa were also taken for histological analysis, while for the qRT-PCR analysis these layers were stripped down. Depending on the time period between septum biopsy and total septum explantation sheep were divided into 2-month and 6-month groups. Every explanted septum was given its identification number and was further divided into newly-formed tissue (NFT) and native sub-samples (Table 3).

Table 3. Two and six-month experimental groups. Within each group, samples were subdivided into newly-formed and native subgroups. During the preparation samples 13 and 14 did not have clearly visible newly-formed tissue part, therefore two samples, that presumably contain newly-formed tissue (NFT), were taken for analysis.

2 MONTHS			6 MONTHS		
Sample ID (NFT)	Sample ID (native)	Sample ID (NFT)		Sample ID (native)	
1	1A	3	15	3A	15A
2	2A	5	16	5A	16A
4	4A	7	18	7A	18A
6	6A	8	20	8A	20A
12	12A	9	22	9A	21A
13 13.2	13A	11		11A	22A
14 14.2	14A				

2.2. Histological and immunohistochemical stainings

2.2.1. Fixation and embedding

Samples collected for histological analysis were put in 4% paraformaldehyde and were left to fixate for one week. Following the dehydration in ascending concentrations of ethanol, samples were immersed in xylene, embedded in paraffin and cut in 5 µm thick sections using microtome.

2.2.2. Deparaffinization and rehydration

Paraffin sections of nasal septum cartilage were deparaffinized and rehydrated by immersing the slides through xylene and ethanol solutions at room temperature (RT). Paraffin was removed by immersing slides in two changes of xylene, 10 minutes each. Subsequently, sections were rehydrated in two changes of 100% ethanol, followed by 96% and 70% ethanol, 5 minutes each. At the end, the section were immersed in distilled water for 5 minutes.

2.2.3. Hematoxylin-eosin staining

After the rehydration, sections were immersed in hematoxylin stain for 5 minutes. The stain was rinsed for 10 minutes in few changes of tap water, dipped two times in acid ethanol, rinsed for 2 minutes in tap water and immersed in ammonia water for 30 seconds. Subsequently, slides were washed for 20 minutes in tap water following with 3 dips in distilled water. Sections were immersed in eosin stain for 60 seconds and rinsed in two changes of 96% ethanol.

2.2.4. Alcian blue staining

Slides were immersed in 1% Alcian blue stain for 30 minutes at room temperature. Subsequently, slides were rinsed in a few changes of distilled water and left to sit in tap water for 10 min. Sections were counterstained by immersing slides in hematoxylin for 3 minutes, followed by washing in 4 changes of distilled water, 5 minutes each.

2.2.5. Collagen type II staining

After deparaffinization and rehydration, sections were washed in distilled water and 1X PBS solution for 5 minutes each. Antigen retrieval was done by incubating sections in 0,1% pronase (Sigma Aldrich, USA) and 2,5% hyaluronidase (Sigma Aldrich, USA) PBS-solutions. The 150 µL/section of pronase was added to slides and incubated in a humidified chamber for 20 minutes at RT. Pronase solution was removed, and 150 µL/section of 2,5% hyaluronidase was added. Slides were incubated in a humidified chamber at 37 °C for 30 minutes. Sections were washed for 5 minutes in 1X PBS, whereupon the blocking was performed. Non-specific antibody binding was blocked by incubation in goat serum (10% in 1X PBS; Dako, Denmark) for 60 minutes at RT. Slides were rinsed for 5 minutes in 1X PBS and wiped around the sections with tissue paper. Sections were incubated with primary anti-collagen type II antibody (1:200 dilution in 1X PBS with 1% goat serum; DSHB, USA) at 4 °C overnight.

Following day, sections were washed in four changes of 1X PBS for 5 minutes each. Sections were incubated in 3% hydrogen peroxide for 10 minutes at RT to block endogenous peroxidase, followed by 5-minute PBS wash. Goat anti-rabbit/mouse HRP conjugated secondary antibody (Dako REAL EnVision Detection system, Agilent) was added to sections and incubated for 30 minutes at RT. Sections were rinsed in six changes of 1X PBS for 5 minutes each. Finally, sections were incubated for 2 minutes at RT with DAB solution (Dako REAL EnVision Detection system, Agilent) prepared by adding Dako REAL DAB+ Chromogen to Dako REAL Substrate Buffer in 1:50 ratio. Detection reaction was terminated by rinsing slides in five changes of distilled water for 2 minutes each. Sections were counterstained with hematoxylin stain for 30 seconds and then rinsed for 5 minutes in distilled water.

2.2.6. Collagen type I staining

Following the deparaffinization and rehydration, slides were put in sodium citrate buffer (10mM sodium citrate, 0.05% Tween 20, pH 6.0) at 60°C overnight. Next morning, slides were left to cool for 15 minutes and were washed in distilled water and 1X PBS solution for 5 minutes each. Additionally, 12-minute incubation with proteinase K (Dako, Denmark) was performed at RT, whereupon slides were rinsed in 1X PBS solution. The following steps were performed similarly to the collagen type II staining protocol but the primary anti-collagen type I antibody (1:500 dilution in 1X PBS with 1% goat serum; Abcam) was used.

2.2.7. Dehydration and mounting

Dehydration for all slides was conducted at RT by immersing slides in graded ethanol (70%, 96%, 100% and 100%) followed by xylene-ethanol solution (1:1) and two changes of xylene for 5 minutes each. Slides were held vertically to drain for a few seconds and then mounted in BioMount New media for covering microscope samples (BioGnost, Croatia).

2.3. Tissue sectioning and cell lysis

The harvested tissue samples intended for gene expression analysis were rectangular in shape containing native and damaged tissue that started to heal (Figure 2.). In order to characterize newly formed tissue in a place of the induced lesion, the samples were sectioned in the manner shown in Figure 2. For every sample, both, native and newly-formed tissue part was taken for further procedures. Following steps were carried out according to Lee et al. (2015), with a few modifications. Briefly, obtained fragments were put on the bottom of small aluminium containers to which 0,5 mL of DEPC water (Sigma Aldrich, USA) was added. The containers were dipped into liquid nitrogen using forceps till the water was fully frozen, after what they were stored at -80 °C. The aluminium container was removed and the ice block with tissue was mounted on the cryostat holder using Tissue Tek (Sakura, Japan). The tissue was cryosectioned into 20 µm sections using Leica CM 1850 cryostat pre-cooled to -20 °C. The first and the last few sections of the native fragment were discarded to eliminate any perichondrium residue. Tissue sections, containing the whole NFT fragment or central part of the native fragment, were collected into 1,5 mL Eppendorf tubes, immediately lysed with 0,5 mL of pre-cooled TRI Reagent (Sigma Aldrich, USA) and stored at -80 °C.

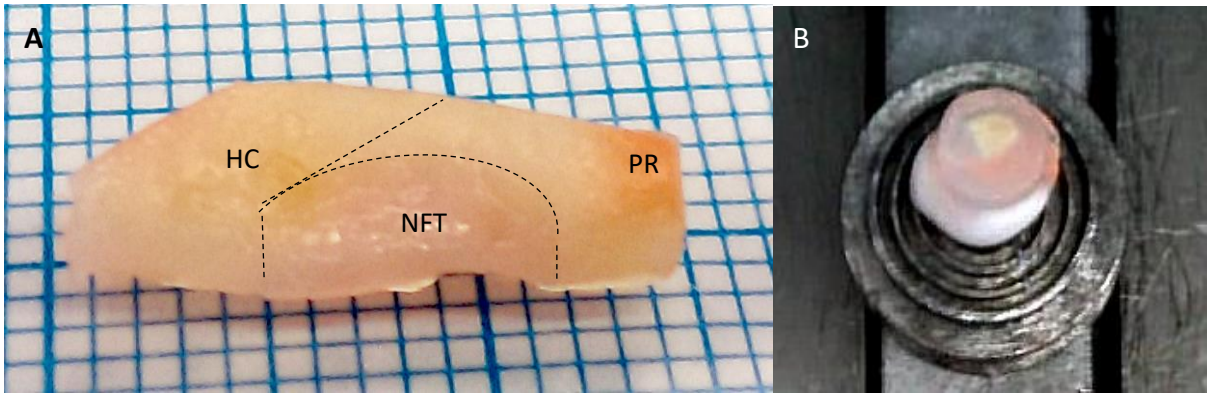

Figure 2. Preparation of the tissue prior cryosectioning A) Harvested cartilaginous nasal septum containing native hyaline cartilage tissue and newly-formed tissue. Perichondrium residues were eliminated during cryosectioning. Dotted lines indicate a place where sectioning was performed. **B)** Ice block with tissue fragment mounted on the cryostat holder using Tissue Tek (Sakura, Japan) HC – hyaline cartilage; NFT – newly-formed tissue; PR – perichondrium residue

2.4. RNA extraction

The total RNA from each sample was isolated from cryosectioned tissue fragments using the TRI Reagent method for RNA isolation as described by Lee et al. (2015). Defrosted tissue sections in 0,5 mL of TRIzol were vortexed for 15 seconds and left to stand for 5 minutes at room temperature (RT). After the addition of 100 µL of chloroform, resulting mixture was again vortexed for 15 seconds, left for 15 min at RT, and centrifuged at 12,000 rpm for 15 minutes at 4 °C on Hettich Universal 320R centrifuge. The aqueous phase was transferred to a fresh tube to which 250 µL of isopropanol and 0,5 µL of glycogen (Roche, Germany) were added. The mixture was vortexed, left to stand for 10 minutes at RT, and centrifuged at 15,000 rpm for 10 minutes at 4 °C. The supernatant was removed, 500 µL of 75% ethanol

was added and centrifuged at 8,000 rpm for 5 minutes at 4 °C with changing the orientation of tubes (the pellet facing towards the centre of centrifuge rotor). The ethanol wash was repeated one more time, whereupon the supernatant was removed and the RNA pellet was left to dry for 10 minutes on ice. After adding 20 µL of DEPC water, tubes were incubated at 60 °C for 10 minutes, vortexed, spun down and stored at -80 °C. RNA concentration and quality were estimated with Nanodrop (Thermo Fisher Scientific, USA).

2.5. DNase treatment and reverse transcription

Isolated RNA was treated with DNase I in order to eliminate any DNA residue. The reaction mixture with a final volume of 20 µL was made according to Table 4 by adding required volumes of DNase I, 10X Reaction Buffer (Thermo Scientific, USA), DEPC water and isolated RNA. The volumes of RNA were adjusted so that each reaction tube contains 1 µg/µL of total isolated RNA. Next, the reaction mixture was vortexed, spun down and incubated at 37 °C for 60 minutes. In order to stop the reaction, 1 µL of EDTA (Thermo Scientific, USA) was added and the resulting mixture was incubated at 65 °C for 10 minutes.

Table 4. The reaction mixture for removal of genomic DNA from RNA preparations (DNase treatment) with a final volume of 20 µL. For each sample, the volume of RNA was calculated from measured concentration to acquire a total of 1 µg RNA per µL of reaction.

Reaction components	Volume (µL)
10X reaction buffer with MgCl2	1
Dnase I, Rnase-free	0,5
DEPC water	$V(DEPC) = 20\mu L - V(RNA)$
RNA	$V(RNA) = \frac{1\ \mu g}{c(RNA)}$

Following the DNase treatment, reverse transcription of total RNA was performed using High Capacity cDNA Reverse Transcription Kit with RNase Inhibitor (Applied Biosystems, USA). The 10 µL of DNase-treated RNA was added to the 10 µL of reaction mixture made according to the manufacturer's instructions. The acquired mixture was left to stand for 10 minutes at RT followed by 120-minute incubation at 37 °C and 5-minute incubation at 85 °C. Resulting cDNA was stored at -20 °C.

2.6. Primer design

Searching through the available scientific publications, characteristic genes for cartilage and perichondrium were found. In order to determine their level of expression in newly-formed tissue qRT-PCR primers were designed. Firstly, corresponding sequences for sheep genes were found in the Ensemble database and borders between exons were determined. Primer design was then performed by setting the optimal parameters for wanted primers in the PrimerQuest (IDT SciTools) setup page. Finally, after choosing the most suitable primers, they were in silico analysed using the AmplifX software (Jullien n.d.). Sequences for GAPDH gene primers were acquired from Garza-Veloz et al. (2013). All of the primers were ordered from Macrogen (LIGO, South Korea). Obtained stock solutions (100 µM) were diluted to working concentration of 10 µM by adding miliQ water. Selected genes with primer sequences and corresponding amplicon lengths are shown in Table 5.

Table 5. Primer sequences, melting temperature (Tm) and expected amplicon length. Melting temperature of each primer pair was adjusted so to be able to perform single PCR run, with elongation temperature of 58°C. *Due to lack of appropriate sequences, primers for CRABP1 gene have slightly imbalanced Tm-s.

Gene	F/R	Primer sequence	Tm (°C)	Fragment length (pb)
COL2	F	GAC AAA GGA GAA ACT GGA GAG	59,4	193
	R	GGA TTC CGT TAG CAC CAT CTT	59,4	
AGG	F	CCC AAC TGA TGC TTC TAT CC	58,4	192
	R	CAC AGC TTC TGG TCA ATC TC	58,4	
COMP	F	GGAA GGA CAA GAC ATC CTA C	60	161
	R	CTG GGA GAA GCA GAA GAC C	60	
COL1A1	F	CAG CAG ATC GAG AAC ATC C	58	165
	R	CTC CAT GTT GCA GAA GAC C	58	
COL4A1	F	GGC TAC TCC TTT GTG ATG C	58	198
	R	GGG CTT CTT GAA CAT CTC G	58	
DKK3	F	GAG GTT GAG GAA CTG ATG G	58	155
	R	ACC TTG GTT TCT GTG TTG G	56	
CRABP1*	F	CAA GTG CAG GAG CTT ACC	56	164
	R	CAT AA TCC TCG TGC AGA CC	60	
GAPDH	F	GAT TGT CAG CAA TGC CTC CT	58,4	194
	R	AAG CAG GGA TGA TGT TTT GG	58,4	

2.7. cDNA quality control

To verify the integrity of the acquired cDNA PCR amplification was performed using primers for the GAPDH, COMP, COL II, AGG, COL I, COL IV, DKK3 and CRABP1 genes (Table 5.). PCR reactions were made according to Table 6 with a final reaction volume of 20 µL. Amplification was performed on Biorad T100 Thermal Cycler according to the programme described in Table 7.

Table 6. The reaction mix for one PCR amplification with a final volume of 20 µL.

Reaction components	Volume (µL)
5X Green GoTaq Reaction Buffer (Promega)	4
GoTaq DNA Polymerase (Promega)	0,1
dNTP mix, 10 mM (Bio Basic Inc.)	0,4
Forward primer, 0.2 µM	0,4
Reverse primer, 0.2 µM	0,4
MiliQ water	12,7
cDNA	2

Table 7. PCR amplification programme

Temperature (°C)	Duration	
95	2 min	
95	30 s	X 38
58	30 s	
72	30 s	
72	5 min	

PCR products were subsequently checked by agarose gel electrophoresis. 1% agarose gel was prepared by adding agarose (Sigma Aldrich, USA) to 1X TAE buffer (40 mM Tris, 20 mM acetic acid, 1mM EDTA) with ethidium bromide (Carl Roth, Switzerland) in a final concentration of 0,5 µg/ml. Quick-Load 50 bp DNA Ladder (New England BioLabs) was used to assess the size of the amplified fragment. The 6 µL of DNA Ladder and 5 µL of the amplified DNA fragment was loaded to the gel and run at 100 V for 20 minutes. Afterwards, the gel was inspected with a Kodak EDAS 290 system.

2.8. Gene expression analysis

To additionally characterise tissue in the place of nasal septum lesion, quantitative Real-Time Polymerase Chain Reaction was performed using both native and newly-formed tissue part of nasal septum tissue as a sample. Reaction mixtures were made according to Table 8 while using primers listed in Table 5. Reactions were performed on a 96-well plate, where all samples were represented in duplicates by adding 1 µL of cDNA to 19 µL of the reaction mixture. Amplification was conducted on the 7500 Fast Real-Time PCR System according to the programme described in Table 9. Gathered data was reviewed and exported using 7500 Software v2.0.6 and analysed using the $\Delta\Delta C_T$ method.

Table 8. The reaction mix for one qRT-PCR amplification with a final volume of 20 µL.

Reaction components	Volume (µL)
Power SYBR Green PCR Master Mix	10
Forward primer, 0.2 µM	0,4
Reverse primer, 0.2 µM	0,4
MiliQ water	8,2
cDNA	1

Table 9. qRT-PCR amplification programme

Temperature (°C)	Duration	
50	20 s	
95	10 min	
95	15 s	X 40
58	1 min	
95	15 s	
60	1 min	
95	30 s	
60	15 s	

2.9. Statistical analysis

In statistics, a T-test is one of the most widely used hypothesis tests that compare the means of two groups. The T-test can be divided into two types. The paired T-test is used when two compared groups are dependent on each other, while unpaired or independent T-test is used for independent groups. When using the unpaired t-test following assumptions for the samples must be satisfied. Examined groups must be mutually independent, whilst the dependent variable should be approximately normally distributed and its variances should be equal. If these criteria are met, the t-score that represents the ratio between the difference between the two groups and the difference within the groups is calculated. Combining calculated degrees of freedom (DF) with given t-scores yields corresponding critical value (CV) to which specific p-value is assigned. Since commonly postulated null-hypothesis is that there is no difference between the groups every t-score higher than CV is considered statistically significant (Tae Kyun 2015). Following the above-mentioned criteria, to test the significance of differences observed in gene expression levels unpaired t-test was performed using Microsoft Excel.

3. RESULTS

3.1. Evaluation of morphological features of newly-formed tissue

To evaluate newly-formed tissue in a place of septum perforation tissue samples were stained with basic histological stains hematoxylin-eosin (H&E) and alcian blue. Hematoxylin-eosin staining is the most commonly used histological staining procedure to asses general tissue morphology (Figure 3 and 4;A,B). It contains eosin which will stain cytoplasmic basic proteins pink and hematoxylin that will stain acidic carbohydrates and nucleus components purple. Upon analysis of H&E stained sections, signs of mucosal tissue were observed, therefore alcian blue staining was performed to estimate the presence of seromucous glands characteristic for this type of tissue (Figure 3 and 4;E,F). It is mainly used to detect mucins, mucopolysaccharides and glycosaminoglycans that stain blue to bluish green. Additionally, for more specific analysis sections were immunohistochemically stained for collagen type I and II. Collagen type II fibres are characteristic for hyaline cartilage, therefore immunostaining for collagen type II showed characteristic cartilage morphology while at the same time indicating incision site (Figure 3 and 4;C). Respectively, collagen type I immunostaining specifically demarked perichondrium and surrounding connective tissue for which collagen type I fibres are characteristic (Figure 3 and 4;D).

Analysis of H&E stained sections showed overall similarity in morphology between two and six-month group. In all of the sections, cartilage was stained purple and incision site could be clearly distinguished. In most of the samples from two-month group cellular aggregation (Figure 3;B) with purplish stained ECM could be noted protruding from the centre of the incision. In a less amount, the same occurrence could be noted throughout six-month group samples (Figure 4;B). Additionally, bright pink stained perichondrium was visible by the sides of the cartilage in all of the samples, bordering with irregular dense connective tissue containing blood vessels and seromucous glands (Figure 3 and 4; B). In the centre of perforation, uniform perichondrium-like tissue with lighter pink colouration could be seen in all of the sections (Figure 4;A). Moreover, some of the samples in both groups had capillaries protruding immediate centre of perforation and in some mucosal tissue has partially invaded the biopsy site (Figure 3;A). Alcialn blue stainings confirmed that in most of the samples there is no mucosal tissue present at the site of perforation (Figure 4;E,F). Although, a small number of samples showed a significant amount of seromucous glands present in the centre of the perforation (Figure 3;F) but not in the vicinity of the cartilage incision (Figure 3;E).

To specifically determine characteristics of newly-formed tissue and to confirm its perichondrium origin, immunohistochemical stainings for collagen type I and II were performed. All of the samples were successfully stained for collagen type II fibres that are cartilage-specific. Common features, including uniformly stained ECM with darker territorial areas, lacunae and isogenous groups of chondrocytes, could be observed (Figure 3 and 4;C). Cell aggregations protruding from the middle of the incision, noted previously in H&E sections, were stained with similar intensity as the native cartilage (Figure 3;C). Still, the difference in cellular content, size and positioning, as well as the ECM appearance is indisputable. The cells seem to be smaller but they are more numerous, while the ECM appears to be less hyaline and irregularly directed. Perichondral origin of the newly-formed tissue at the site of perforation was confirmed through collagen type I immunostaining. In every sample, perichondrium had the fibrillar appearance and was stained brown. The same looking tissue could be found surrounding the site of the incision as well as throughout the perforation (Figure 3 and 4;D). Surrounding dense connective tissue was also stained as collagen type I is the major component of all connective tissues, but morphology was clearly distinguishable. Interestingly, previously mentioned cellular aggregations were also stained for collagen type I (Figure 3 and 4;D), presumably indicating the invasion of perichondral cells into the aggregation.

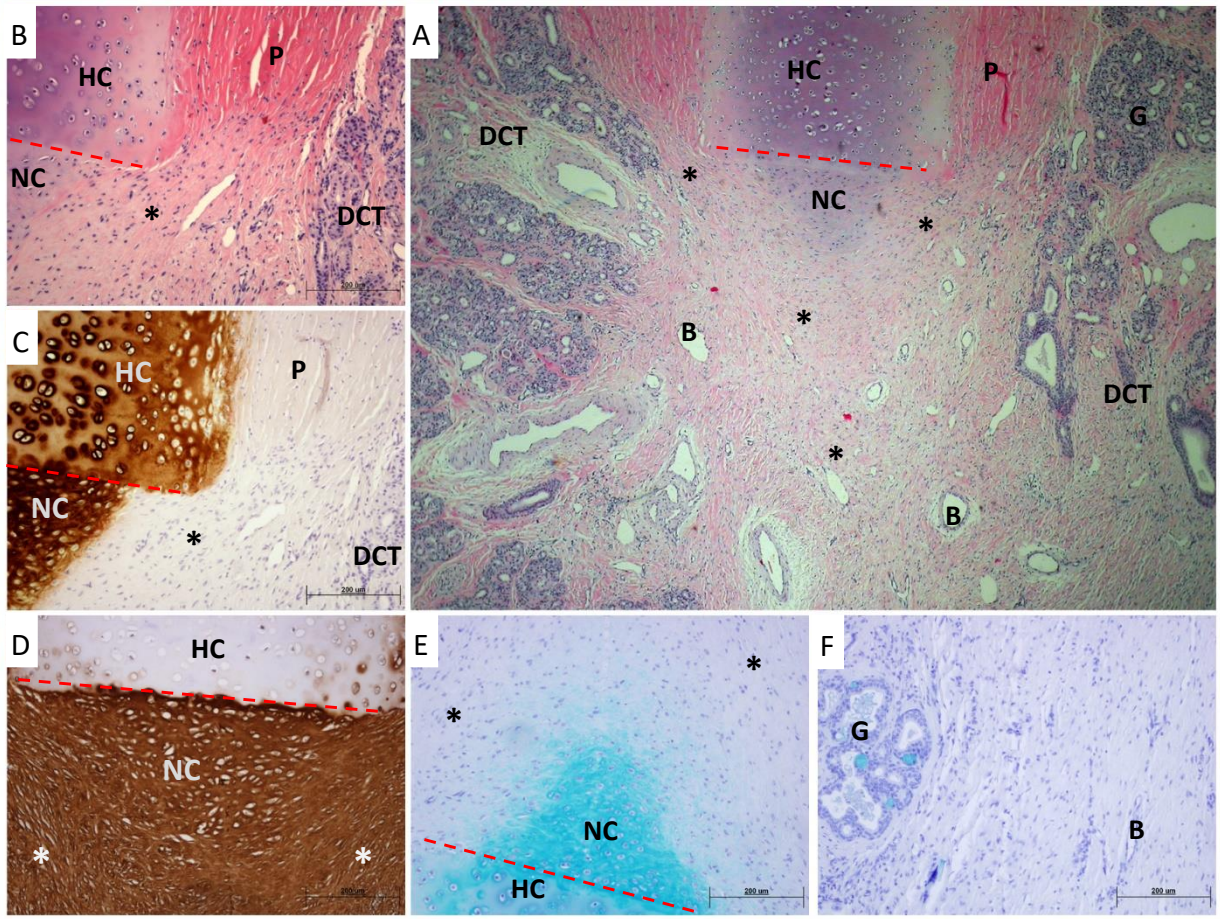

Figure 3. Histological stainings of sheep (ID 12423) nasal septum sample (2-month biopsy). Asterisks (*) indicate sites of outgrowth, and ingrowth on the place of the perforation, red dashed line indicates the place of incision **A) Hematoxylin-eosin staining, 4x magnification** – hyaline cartilage with perichondrium overgrowing its edges and the neocartilage. Closer to the middle of the perforation perichondrium-like tissue becomes intertwined with mucosal tissue. By the sides of the perichondrium, irregular dense connective tissue with blood vessels and seromucosal glands can be noted. **B) Hematoxyline staining, 10x magnification** – hyaline cartilage with its characteristic morphology is stained dark purple while the neocartilage is stained lighter indicating ongoing accumulation of cartilage ECM components. Perichondrium, which is visible by the sides of the cartilage and is stained bright pink, overgrows the edges of native cartilage and continues to protrude into the site of perforation. **C) Collagen type II immunostaining, 10x magnification** – brown colouration of hyaline cartilage with characteristic morphology and neocartilage with higher cellular content and less hyaline matrix appearance. **D) Collagen type I immunostaining, 10x magnification** – perichondrium is specifically stained brown almost the same as neocartilage, suggesting protrusion of perichondrium cells into neocartilage tissue. **E) Alcian blue staining, 10x magnification** – due to high glycoprotein content cartilage is stained bright blue but no mucopolysaccharides aggregations are notable **F) Alcian blue staining, 10x magnification (centre)** – the centre of perforation is filed by perichondrium-like tissue. By the sides, mucosal tissue can be found with characteristic bright blue staining of mucopolysaccharides in seromucous glands. HC – native hyaline cartilage; NC – neocartilage; P – perichondrium; DCT – irregular dense connective tissue; B – blood vessels; G – seromucous glands

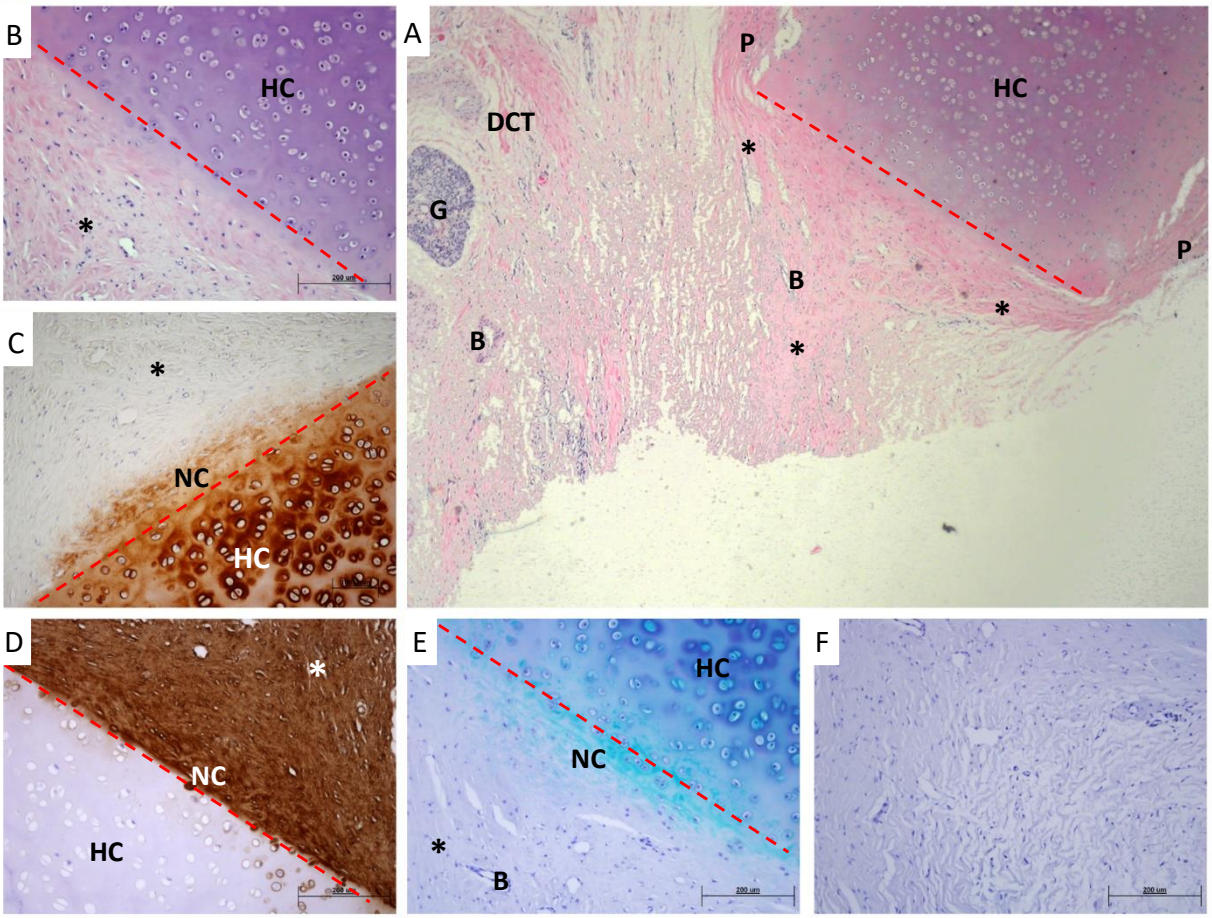

Figure 4. Histological stainings of sheep (ID 28519) nasal septum sample (6-month biopsy). Asterisks (*) indicate sites of outgrowth, and ingrowth on the place of the perforation, red dashed line indicates the place of incision **A) Hematoxylin-eosin staining, 4x magnification** – hyaline cartilage with perichondrium overgrowing its edges and the neocartilage. Approaching the middle of the perforation perichondrium-like tissue becomes intertwined with mucosal tissue in some samples. By the sides of the perichondrium, irregular dense connective tissue with blood vessels and seromucosal glands can be noted. **B) Hematoxyline staining, 10x magnification** – hyaline cartilage with its characteristic morphology is stained dark purple. Perichondrium overgrows the edges of native cartilage and continues to protrude into the site of perforation. **C) Collagen type II immunostaining, 10x magnification** – brown colouration of hyaline cartilage with characteristic morphology and a small portion of neocartilage with less hyaline matrix appearance. **D) Collagen type I immunostaining, 10x magnification** – perichondrium is specifically stained brown in the same manner as neocartilage, suggesting protrusion of perichondrium cells into neocartilage tissue. **E) Alcian blue staining, 10x magnification** – due to high glycoprotein content cartilage is stained bright blue but no mucopolysaccharides aggregations are notable **F) Alcian blue staining, 10x magnification (centre)** – the centre of perforation is filed by perichondrium-like tissue with minimal indication of mucosal tissue protruding the perforation site. HC – native hyaline cartilage; NC – neocartilage; P – perichondrium; DCT – irregular dense connective tissue; B – blood vessels; G – seromucous glands

3.2. Primer specificity

Since most of the primers for PCR and qPCR amplifications were designed using appropriate software and ordered from Macrogen, their effectiveness and specificity had to be proven. Considering that PCR amplified gene fragments had expected size (Table 5, Figure 6-8), and no other unspecific fragments could be detected primers were considered to be effective and specific. Additionally, these conclusions were confirmed by reviewing melt curves obtained during qPCR amplifications (Figure 5). For every gene, amplified fragments show just one peak, meaning, primers specifically amplify desired gene fragment.

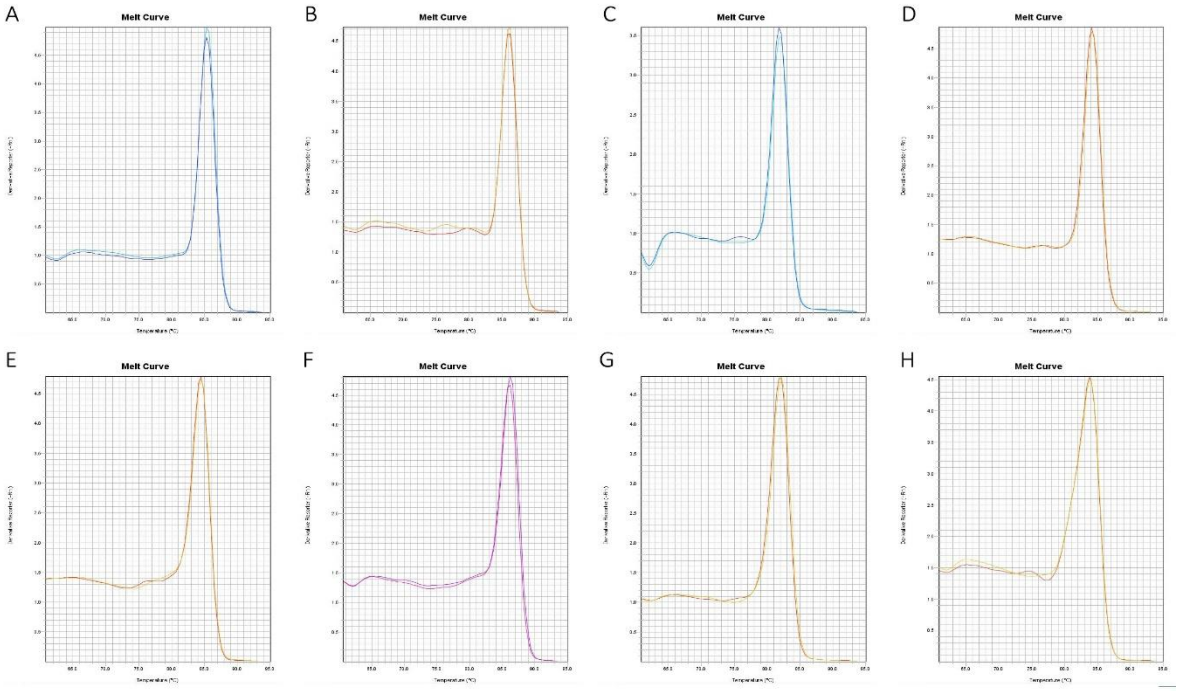

Figure 5. Melt curves of A) GAPDH, B) COL 2, C) AGG, D) COMP, E) COL 1, F) COL 4, G) DKK 3 and H) CRABP 1 PCR amplicons. All amplicons exhibit one peak in a temperature range from 82°C to 86°C, indicating primer specificity.

3.3. cDNA integrity validation

For RNA isolation TRI reagent method was exploited after grinding tissue by cryosectioning, as it was found that it yields RNA with the best quality. Following the reverse transcription of total RNA to cDNA, PCR amplification was performed to asses cDNA integrity and also to acquire insight into gene expression prior to qPCR reactions. Fragment of GAPDH gene from cDNA of both NFT and native part of nasal septum was amplified (Figure 6) as it was to be used as endogenous control in qPCR reactions. For newly-formed tissue part characteristic gene (COL1, COL4, DKK3 and CRABP1) fragments were amplified (Figure 7), as well as for native part (COL2, AGG and COMP; Figure 8).

Samples 5, 7, 9, and 11 were shown to be least preserved and therefore were not taken into consideration for further analysis. They had low-intensity markings for GAPDH gene fragment, as well as for most of the other relevant genes. These findings were in concordance with low RNA concentrations and integrity, hence it was not expected they will give any results in qPCR analysis. All other samples had GAPDH marking of similar intensity but differed for other relevant genes. However, they were included in the qPCR analysis as the differences in other genes may be due to differentially expressed genes in individual samples.

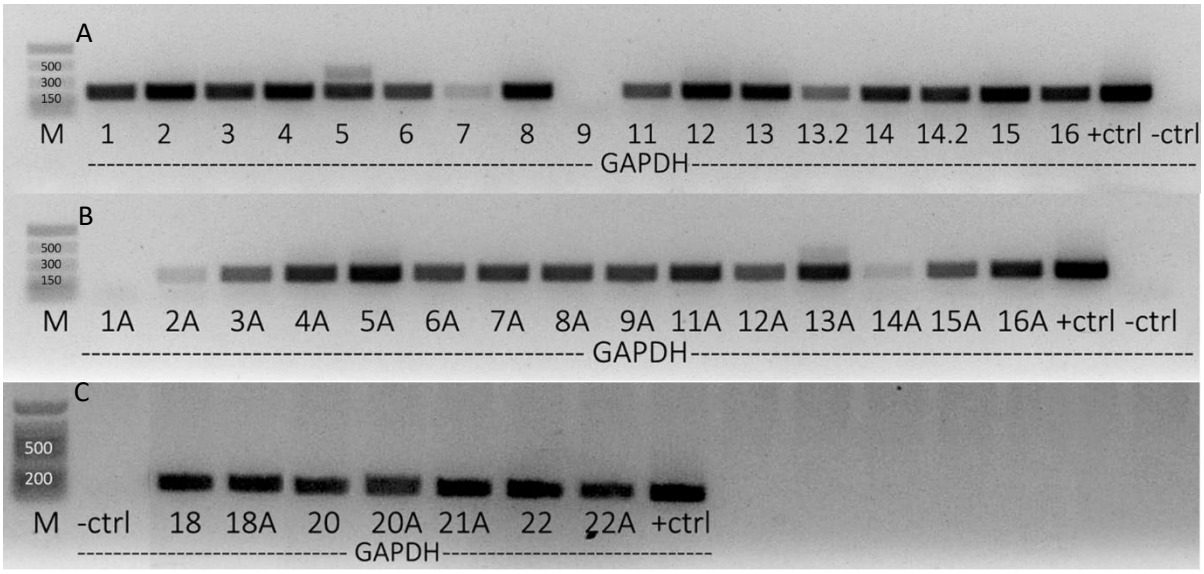

Figure 6. Amplified fragments of GAPDH gene for both newly-formed tissue (NFT) and native septum specimens. PCR was performed with specific primers and cDNA as a template. **A) NFT specimens of samples 1-16** – there are two specimens for samples 13 and 14 as the newly-formed site was not clearly visible during the preparation. Samples 5, 7, 9 and 13.2 have lower quality than the others. **B) Native specimens of samples 1-16** – samples 1A, 2A and 14A have lower quality, whereas 5A and 16A show the highest intensity. **C) NFT and native specimens of samples 18-22** – a newly-formed part of sample 21 was not visible during preparation and therefore is not included in expression analysis. All other specimens show similar intensity meaning they have similar quality.

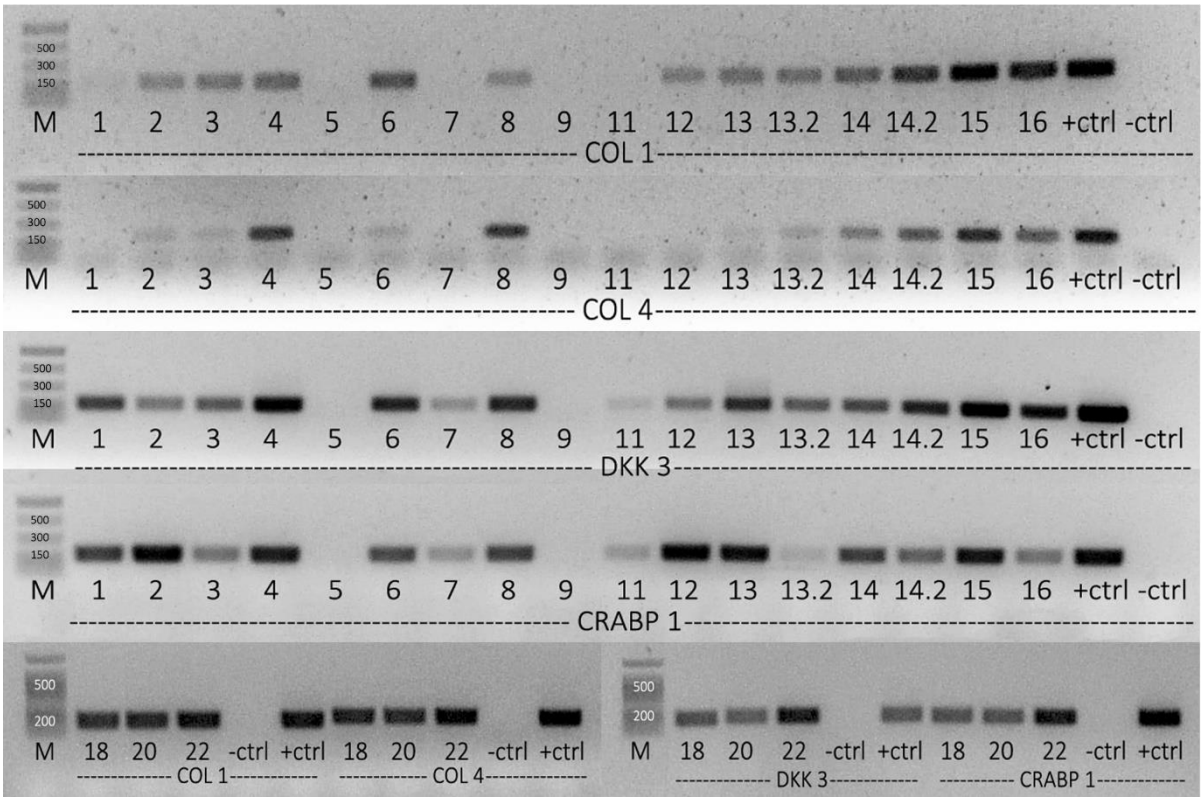

Figure 7. Amplified fragments of genes characteristic for newly-formed tissue (NFT) septum specimens. PCR was performed with specific primers and cDNA as a template. In most of the samples, all of the characteristic genes are evident. Samples 5, 7, 9, and 11 exhibit faint or no markings for any of the amplified gene fragments indicating poor cDNA quality.

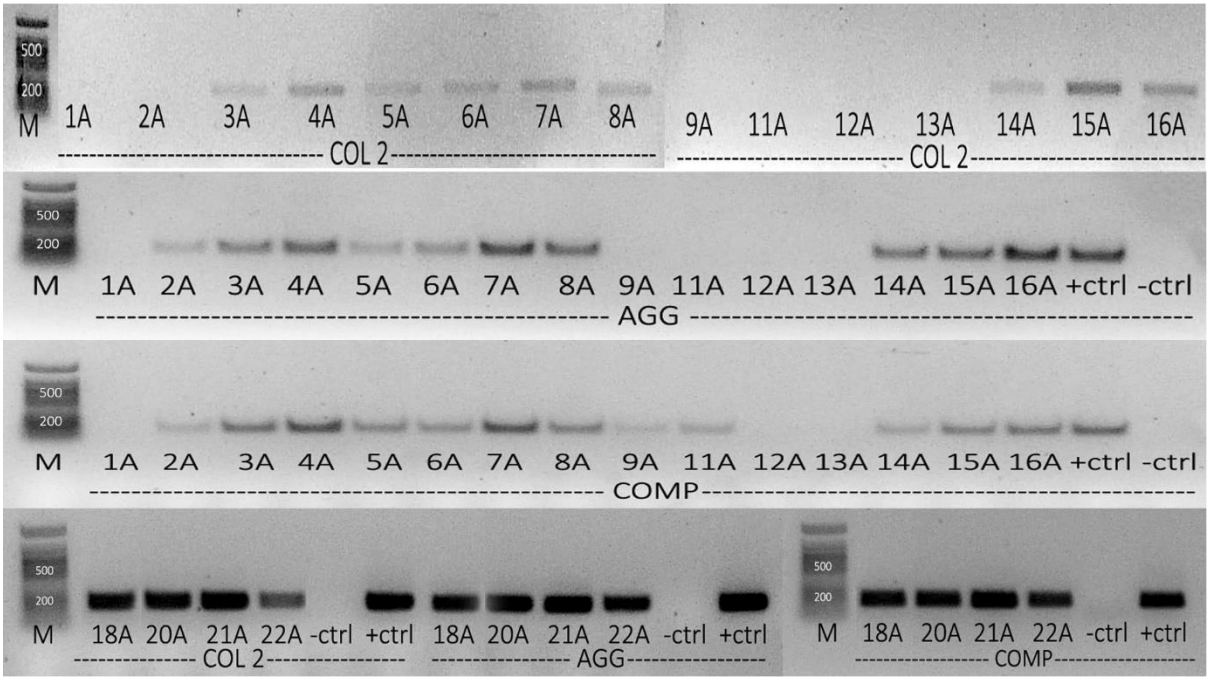

Figure 8. Amplified fragments of genes characteristic for native septum specimens. PCR was performed with specific primers and cDNA as a template. In most of the samples, the expression of characteristic genes is evident. Samples 1A, 9A, 12A and 13A exhibit no markings for any of the amplified gene fragments indicating poor cDNA (hence RNA) quality.

3.4. Gene expression analysis of cartilage and perichondrium markers

Following the PCR analysis, satisfying samples were further used for gene expression analysis through qPCR. Housekeeping gene GAPDH was used as endogenous control while native specimens were used as a control (commonly known as untreated) group. Following the amplification, resulting data was analysed using the $\Delta\Delta C_T$ method which yields relative gene expression in a given sample. Expression of tissue-specific genes was examined with COL 2, AGG and COMP genes as cartilage-specific, and COL1, COL 4, DKK 3, and CRABP 1 as perichondrium specific. Moreover, perichondrium specific genes were selected with the purpose of distinguishing the inner and outer perichondrium layer. Therefore, DKK 3 was chosen as an inner layer marker, while COL 4 and CRABP 1 serve as outer layer markers. Collagen type 1 (COL 1) is widely present in all connective tissues, but its content is significantly higher in perichondrium, hence it was selected as general perichondrium marker.

Gene expressions of samples from both two-month (Figure 9.) and six-month (Figure 10.) group were compared to native cartilage control samples. In a control group, higher expression levels of cartilage characteristic genes COL 2, AGG and COMP is evident, whereas in both test groups expression of these genes is reduced. On the contrary, perichondral marker genes had elevated expression levels in both test groups and were lowered in the control group. Following the calculations, the difference in native and newly-formed tissue observed through histological analysis was confirmed. Significant differences in relative gene expression between native cartilage and newly-formed tissue could be observed in both test groups (Unpaired t-test; DF=10; p=0,05-0,01), with exception of DKK 3 and COL 1 genes. Higher expression of COL 1, COL 4 and CRABP 1 genes indicate the direct role of outer perichondrium layer in the formation of new tissue at the site of perforation. Differences in tissue expression of DKK 3 gene were found to be statistically irrelevant suggesting that inner perichondrium layer has no effect on the formation of new tissue. Also, in the six-month group, there were no significant differences in COL 1 expression between native and newly-formed tissue. However, both of these observations may be due to perichondrium residues in native tissue samples or insufficient precision during separation of newly-formed tissue from the native cartilage.

When comparing two test groups (Figure 11) no significant difference was observed. Still, expression levels of perichondral markers significantly differed from those of cartilage markers within newly-formed tissue (Unpaired t-test; DF=10; p=0,05-0,01). Cartilage marker genes retain their low expression level as the time passes, confirming cartilage inability to regenerate. In both test groups, high expression of perichondral markers can be observed, as well as an increase in expression level over time. Although, the difference is not statistically significant it does suggest the possibility of higher expression levels in newly-formed tissue over a longer period of time. However, expression of COL 4 gene does not follow this increasing trend, what may be, as well as DKK 3 and COL 1 deviations, explained by unprecise sample handling.

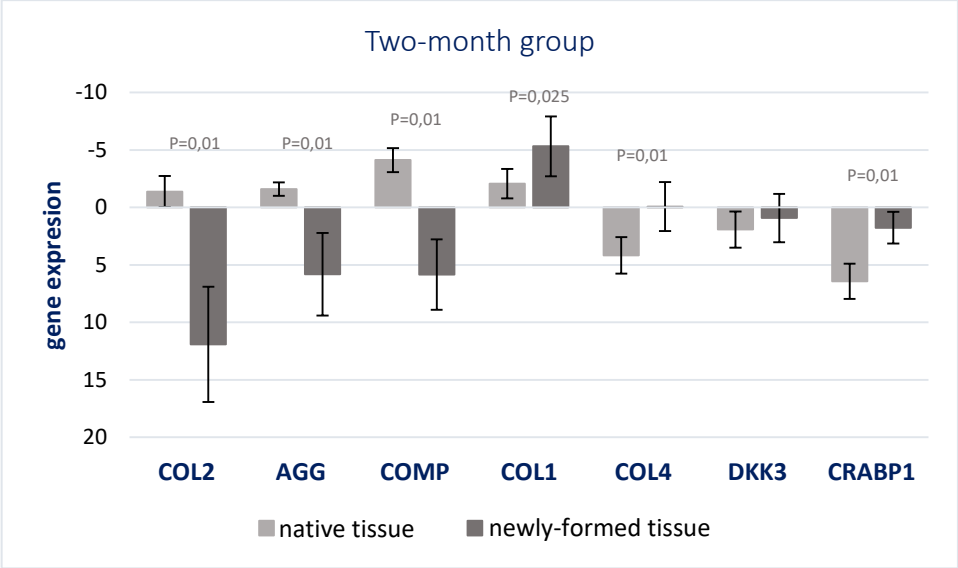

Figure 9. Relative gene expression in two-month group newly-formed tissue samples compared to the control group (native tissue). qPCR was performed with specific primers and results were expressed as ΔC_T values. COL2: Collagen type II, AGG: Aggrecan, COMP: Cartilage oligomeric matrix protein, COL1: Collagen type I, COL4: Collagen type IV, DKK3: Dickkopf WNT Signaling Pathway Inhibitor 3, CRABP1: Cellular Retinoic Acid Binding Protein-I. Unpaired t-test; DF=10; p=0,025-0,01.

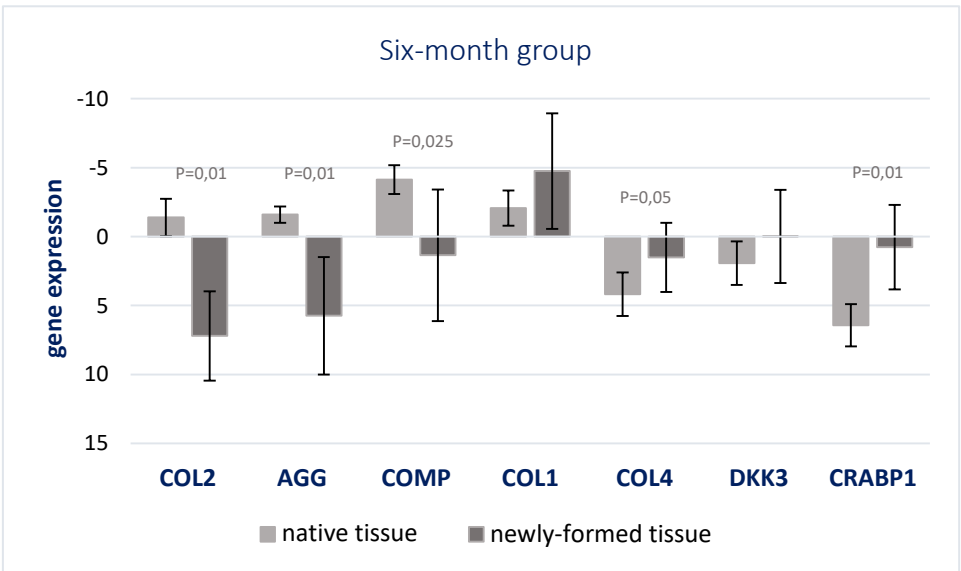

Figure 10. Relative gene expression in six-month group newly-formed tissue samples compared to the control group (native tissue). qPCR was performed with specific primers and results were expressed as ΔC_T values. COL2: Collagen type II, AGG: Aggrecan, COMP: Cartilage oligomeric matrix protein, COL1: Collagen type I, COL4: Collagen type IV, DKK3: Dickkopf WNT Signaling Pathway Inhibitor 3, CRABP1: Cellular Retinoic Acid Binding Protein-I. Unpaired t-test; DF=10; p=0,05-0,01.

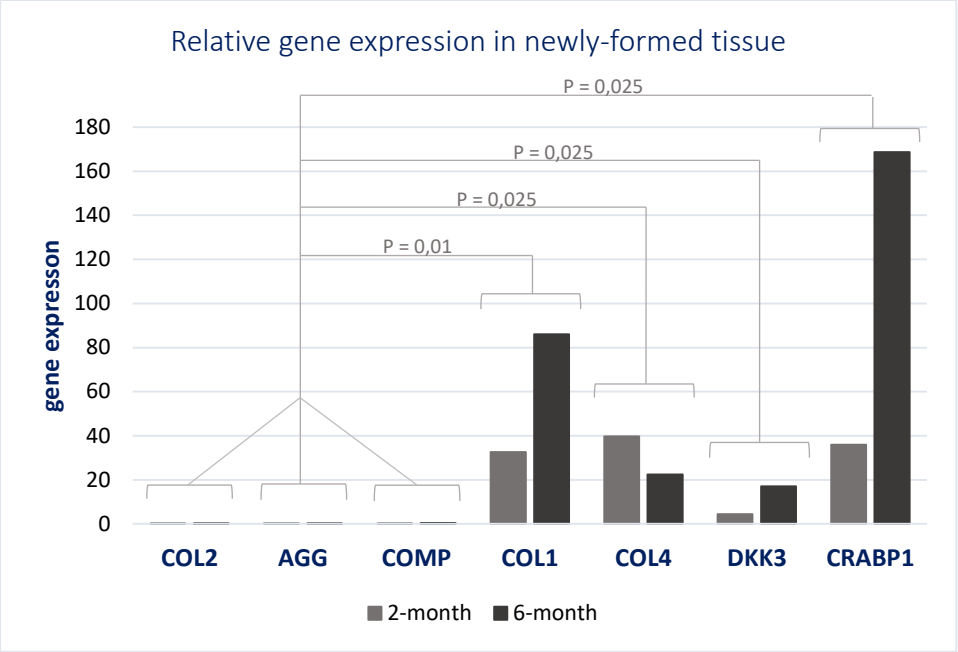

Figure 11. Comparison of relative gene expression between the two-month and six-month group. qPCR was performed with specific primers and results were expressed as Fold Change (FC) values. COL2: Collagen type II, AGG: Aggrecan, COMP: Cartilage oligomeric matrix protein, COL1: Collagen type I, COL4: Collagen type IV, DKK3: Dickkopf WNT Signaling Pathway Inhibitor 3, CRABP1: Cellular Retinoic Acid Binding Protein-I. Unpaired t-test; DF=10; p=0,025-0,01.

4. DISCUSSION

Advances in the field of tissue engineering have brought to sight new treatment possibilities for cartilage injuries and chronic diseases such as osteoarthritis. Many efforts are made to introduce new treatments into the clinic hence a large number of pre-clinical studies on large animal modes are conducted. The overall goal is to produce tissue grafts using optimal cell source and scaffolds as well as to achieve integration into native tissue and accelerate the healing process. One such procedure already found its way to the clinic. In this procedure, autologous chondrocytes are harvested from the nasal septum, expanded *in vitro* and seeded on 3D collagen scaffold to produce cartilage tissue implants. Engineered tissue is implanted directly to the injury site where it facilitates the healing process (Mumme et al. 2016b). Biopsy of nasal septum enables quick and easy chondrocyte harvest but produces perforation that fills in over time. To this time, no one has addressed the issue of tissue formation in the place of the perforation on large animal model. The newly-formed tissue may not possess functional properties characteristic for septum cartilage, whereas if the neocartilage formes it would enable chondrocyte reharvesting and confirm normal septum function. Hence, the overall aim of this thesis was to characterize tissue formed on the perforation site, on large animal sheep model, by examining tissue morphology and gene expression.

Histological stainings of tissue sections revealed general appearance and tissue structure. Both samples from two-month (Figure 3.) and six-month (Figure 4.) test group show similar morphology characteristics. Septum cartilage with perichondrium by its sides was not affected by the procedure, and incision site could be clearly distinguished through all of the samples. The incision was made both through cartilage and perichondrium, as in sheep model perichondrium is tightly bound to the septal cartilage. Also, by the sides of intact perichondrium, lamina propria with various cell types, blood and lymph vessels and seromucous glands was present in all samples. These characteristic features of intact nasal septum cartilage and surrounding tissue are in consensus with previous research (Bleys et al. 2007). At the perforation site, differing tissue morphology was observed even with the basic H&E staining (Figure 3 and 4; A,B), as there were no indicators of cartilaginous tissue. As it was previously established, collagen type II fibres are exclusively present in cartilage tissue while collagen type I fibres are abundant in perichondrium and are not evident in native cartilage (Popko et al. 2007; Aksoy et al. 2012). Therefore, immunostaining against collagen type II (Figure 3 and 4;C) and collagen type I (Figure 3 and 4;D) confirmed that newly-formed tissue was not of cartilage origin but rather perichondral. The intrusion of fibrous-looking perichondrium from the sides of intact cartilage towards the middle of the incision and further into the perforation site was clearly visible throughout all staining procedures. In most of the samples, perichondrium-like tissue protruded from both sides of the biopsy edges, joining in the centre of the perforation, while dense connective tissue of lamina propria extended by its sides. Alcian blue staining showed seromucous glands invading perichondrium-like tissue in minority of samples (Figure 4;E) whereas only two samples showed perforation completely filled with mucosal tissue.

Evidence of neocartilage formation following the induced lesion in rabbit model are presented in some studies. Neocartilage tissue with characteristic immature appearance was detected in young rabbit model 4 weeks after lesion introduction. However, this was the case only if perichondrium was lifted from the cartilage and laid back following the cartilage biopsy (Skoog et al. 1972). These observations were later confirmed by Kaiser et al. (2006) in adult rabbit model where neocartilage with several cartilage proliferation centres was described. Tissue with similar characteristics was observed in almost every sample examined within this research. Small, densely packed cells surrounded by a matrix that stains positive for collagen type II, were found extending from the native cartilage at the incision site (Figure 3 and 4;C). Their morphology and matrix content indicate increased proliferation rate, therefore the formation of new cartilage tissue. These cell aggregations were found to be more pronounced two months (Figure 3;C) after the biopsy while six months after they could be seen as a thin line bordering the

native cartilage (Figure 4;C). Interestingly, except for staining positively for collagen type II, they also stained positively for collagen type I (Figure 3 and 4;D), possibly due to opposing signalling from the surrounding tissue that drove some cells to produce collagen type I fibres. Verwoerd-Verhoef et al. (1998) described similar looking neocartilage tissue formed after perpendicular cartilage transsection in a rabbit model. The neocartilage with multiple mitoses was described as a triangularly shaped tissue covered by perichondrium and separated from the septum cartilage by a demarcation zone of necrotic tissue. However, mentioned observations were made on animals younger than sheep in this study, and precise explanation of surgical procedures was not given. Even though it is tempting to describe detected cell aggregations as newly-formed cartilage, they are more likely result of errors during the biopsy procedure. Still, non of this explanations regard positive collagen type I staining of these aggregations, therefore further investigation would be desirable to shed a light on these occurrences.

Moreover, the existence of two perichondral layers with distinct features and functions has been described by Bleys et al. (2007). Following the perichondrium and cartilage injury, outer fibrous layer covers the cut edge subsequently preventing induction of cartilage regeneration by inner cambium layer (Duynstee et al. 2002). Fibrous-looking tissue extending from perichondrium towards the middle of perforation was present in almost every sample in both test groups. One sample in each group had perforation filled by surrounding dense connective tissue with abundant glands, blood and lymph vessels. To confirm the outer layer origin of the newly-formed tissue gene expression of several genes was examined by the qPCR method. Presence of collagen type II in hyaline cartilage, and collagen type I abundance in perichondrium were established in many publications (Popko et al. 2007; Bleys et al. 2007; Aigner et al. 1993; Bairati et al. 1996). Lately, detection of more specific perichondrium markers became more interesting subject due to perichondral cell contamination in tissue engineering procedures. Many potential candidates were found (Bandyopadhyay et al. 2008; Hinton et al. 2009; Späth et al. 2018), from which COL 4, DKK 3 and CRABP 1 genes were chosen for the purposes of this study.

Gene expression analysis confirmed that biopsy made perforation becomes filled mainly by perichondrium-like tissue. Both, two and six months after the biopsy low or nonexistent expression of cartilage marker genes was observed in newly-formed tissue obviously disputing any chondrogenic activity in this area (Figure 9, 10 and 11.). Low expression of these genes can be ineluctably attributed to unprecise sample handling while separating newly-formed and native tissue parts. Furthermore, in the native tissue control group, these genes expectedly had elevated expression rates, what is consecutive with previous findings (Nathaniel et al. 1998; Fox et al. 2009; Hinton et al. 2009). Perichondrium markers, except DKK 3 gene, exhibited significantly elevated expression rates in newly-formed tissue compared to the native cartilage. Collagen type I, as a general perichondrium marker, was found to be highly expressed in samples from both time points compared to the control tissue. Still, no statistical relevance of collagen type I expression was noted between two and six-month time point, however, this is most likely due to errors in sample handling. Cartilage has significantly lower cellularity than surrounding perichondrium, so even slightest perichondrium residue in native cartilage control samples may lead to significant changes in gene expression patterns. High expression was also recorded for collagen type IV gene whose protein products are components of extracellular matrix most abundantly found in basement membranes. There, they interact with other ECM components and play a role in cell migration, growth and survival. Even though collagen type IV is present in cartilage (Foldager et al. 2014) it is still one of the genes with highest expression difference when comparing developing perichondrium and cartilage (Späth et al. 2018). Given its role in the assembly and maintaining ECM structure, COL 4 may be relevant during healing process whereas its expression is to be elevated. Conclusively, increased expression of COL I and IV within newly-formed tissue, as well as compared to the native cartilage unquestionably confirmes histologic observations that the perforation in septal cartilage fills in with tissue of perichondral origin.

Furthermore, DKK 3 and CRABP 1 genes were found to be specifically located to the inner and outer perichondrium layer, respectively (Bandyopadhyay et al. 2008). Although DKK 3 was primarily found in perichondrium, some cells resigning in the cartilage periphery were also found expressing this gene. As

inner perichondrium layer has been proposed to participate in appositional cartilage growth it was suggested that DKK 3 expressing cells migrate from perichondrium and aid cartilage growth. The CRABP 1 expressing cells were detected in outer perichondrium layer where they respond to retinoic acid signalling. The protein product of CRABP 1 gene is a molecule with a role in RA trafficking that subsequently, results in negative regulation of cartilage growth (Eames, De la Fuente, and Helms 2003). Concordantly, CRABP 1 expression was noted as elevated in newly-formed tissue while DKK 3 expression was not significantly different from its expression in native cartilage (Figure 9, 10 and 11.). Together, these observations confirm the earlier described role of outer perichondrium layer in the production of fibrous tissue following cartilage injury (Duynstee et al. 2002).

Even though every chosen perichondrium characteristic gene had significantly higher expression rate in newly-formed, perichondrium-like tissue compared to native cartilage, their mutual differences were not as pronounced. Within newly-formed tissue, all perichondrium markers had significantly higher expression than cartilage markers (Figure 11.). This remained unchanged over time as the similar trend was noted in samples taken six months after biopsy. Although, completely filled out perforation site could be macroscopically observed at the six-month time point, the difference in gene expression between samples harvested two and six months after biopsy was not statistically significant. Such an occurrence should not be surprising as all of the chosen genes are final products that characterize fully formed mature tissue. For research-oriented on time-related changes during new tissue formation genes involved in cell signalling, differentiation, migration and proliferation may provide more relevant results.

Finally, it is safe to say that a combination of histological tissue analysis and qPCR gene expression analysis yields results that complement each other. Overall observations made after histological staining procedures provide basic insight into tissue morphology and possible relations. On the contrary, gene expression analysis enables precise and more specific tissue characterization through characteristic marker genes, as it can unambiguously determine cell or tissue type. Still, it is highly sensitive and dependant on sample processing and quality of isolated RNA. Sometimes, even the smallest errors during tissue preparation can lead to altered or false results. Within this research, both methods were exploited to describe tissue formed at the nasal septum perforation site. Both histology and gene expression analysis confirmed the perichondral origin of newly-formed tissue while histological slides revealed signs of seromoucosal glands (characteristic for lamina propria) invading perichondrium-like tissue. Additional qPCR gene expression analysis with genes characteristic for lamina propria could be conducted to comprehend this occurrence and to additionally confirm histological observations. Gene expression analysis did not show a significant difference between DKK 3 and CRABP 1 genes, hence could not determine which perichondrium layer plays the main role in new tissue development. However, from histological slides was more than evident that newly-formed tissue had fibrous morphology. Even though the new tissue is not cartilaginous, it still may have sufficient properties to support normal septum function. An interesting follow-up would be to examine the perforation site at a further time point to determine long-term changes in formed tissue as well as its functional properties and possible morbidity. Also, study with a larger sample size should be conducted to additionally confirm the above-mentioned observations.

5. CONCLUSION

This study for the first time describes newly-formed tissue after nasal septum biopsy in a large animal pre-clinical model. Once again, low regenerative potential of cartilaginous tissue was confirmed as the induced perforation was filled with perichondrium-like tissue. Histological analysis showed unchanged cartilage incision site grownover with perichondrium-like tissue that protrudes into te perforation site. Morphologically tissue retains its characteristics over a half year period. Gene expression analysis confirmed the perichondral origin of newly-formed tissue as all marker genes exibited elevated expression levels compared to cartilage markers and native cartilage. Additionally, collagen type I showed to be the most stabile perichondrium indicator and was confirmed as a wide used perichondrium marker. Although, outer layer involvement in new tissue formation could be seen from histological analysis significant difference between inner and outer layer markers within new tissue was not recorded through qPCR method. Still, comparing to cartilage tissue outer layer marker, CRABP 1, was significantly higher, confirming the prevalence of outer layer tissue. Conclusively, tissue formed after the biopsy originates from perichondrium tissue and most certainly differs from native septum cartilage, hence it may not exhibit the same functional properties. Further studies remain to be conducted to fully reveal consequences subsequent to nasal septum biopsy.

6. REFERENCES

Aigner, Thomas, Wolf Bertling, Hartmut Stoss, Gerd Weseloh, and Klaus von der Mark. 1993. "Independent Expression of Fibril-Forming Collagens 1, 11, and III in Chondrocytes of Human Osteoarthritic Cartilage." *Journal of Clinical Investigation* 91:829–37.

Aksoy, F., Y. S. Yildirim, H. Demirhan, O. Özturan, and S. Solakoglu. 2012. "Structural Characteristics of Septal Cartilage and Mucoperichondrium." *Journal of Laryngology and Otology* 126(1):38–42.

Ali, S. Yousuf et al. 1983. *Cartilage Structure Function and Biochemistry*. edited by B. K. Hall. New York: Academic Press.

Archer, Charles W. and Philippa Francis-West. 2003. "The Chondrocyte." *International Journal of Biochemistry and Cell Biology* 35(4):401–4.

Bairati, A., M. Comazzi, and M. Gioria. 1996. "An Ultrastructural Study of the Perichondrium in Cartilages of the Chick Embryo." *Anatomy and Embryology* 194(2):155–67.

Bandyopadhyay, Amitabha, James K. Kubilus, Marsha L. Crochiere, F. Thomas, and Clifford J. Tabin. 2008. "Identification of Unique Molecular Subdomains in the Perichondrium and Periosteum and Their Role in Regulating Gene Expression in the Underlying Chondrocytes." *Dev Biol.* 321(1):162–74.

Bleys, Ronald L. A. W., Mariola Popko, Jan Willem De Groot, and Egbert H. Huizing. 2007. "Histological Structure of the Nasal Cartilages and Their Perichondrial Envelope. II. The Perichondral Envelope of the Septal and Lobular Cartilage." *Rhinology* 45:153–57.

Chu, Constance R., Michal Szczodry, and Stephen Bruno. 2010. "Animal Models for Cartilage Regeneration and Repair." 16(1).

Cook, J. L. et al. 2014. "Animal Models of Cartilage Repair." 3(4):89–94.

Cooper, Geoffrey M. and Robert E. Hausman. 2016. *The Cell: A Molecular Approach*. 7th ed. edited by C. Holabird. Sinauer Associates.

DeLise, A. M., L. Fischer, and R. S. Tuan. 2000. "Cellular Interactions and Signaling in Cartilage Development." *Osteoarthritis and Cartilage* 8(5):309–34.

Duynstee, Mark L. G., Henriette L. Verwoerd-Verhoef, Carel D. A. Verwoerd, and Gerjo J. V. M. Van Osch. 2002. "The Dual Role of Perichondrium in Cartilage Wound Healing." *Plastic and Reconstructive Surgery* 110(4):1073–79.

Eames, B. Frank, Luis De la Fuente, and Jill A. Helms. 2003. "Molecular Ontogeny of the Skeleton." *Birth Defects Research Part C - Embryo Today: Reviews* 69(2):93–101.

Farach-Carson, Mary C., Roger C. Eagner, and Kristi L. Kiick. 2007. "Extracellular Matrix: Structure, Function, and Applications to Tissue Engineering." P. 3.1-3.22 in *Tissue Engineering*, edited by J. P. Fisher, A. G. Mikos, and J. D. Bronzino. Boca Raton: CRC Press.

Farhadi, Jian et al. 2006. "Precultivation of Engineered Human Nasal Cartilage Enhances the Mechanical Properties Relevant for Use in Facial Reconstructive Surgery." *Annals of Surgery* 244(6):978–85.

Foldager, Casper Bindzus, Wei Seong Toh, Andreas H. Gomoll, Bjørn Reino Olsen, and Myron Spector. 2014. "Distribution of Basement Membrane Molecules, Laminin and Collagen Type IV, in Normal and Degenerated Cartilage Tissues." *Cartilage* 5(2):123–32.

Fox, Alice J. Sophia, Asheesh Bedi, and Scott A. Rodeo. 2009. "The Basic Science of Articular Cartilage: Structure, Composition, and Function." *Sports health* 1(6):461–68.

Garza-Veloz, Idalia et al. 2013. "Analyses of Chondrogenic Induction of Adipose Mesenchymal Stem Cells by Combined Co-Stimulation Mediated by Adenoviral Gene Transfer." *Arthritis Research and Therapy* 15(4):R80. Retrieved (http://arthritis-research.com/content/15/4/R80).

Goldring, Mary B., Kaneyuki Tsuchimochi, and Kosei Ijiri. 2006. "The Control of Chondrogenesis." *Journal of Cellular Biochemistry* 97(1):33–44.

Grassel, Susanne and Attila Aszodi, eds. 2016. *Cartilage: Volume 1: Physiology and Development*. Springer.

Hinton, RJ, M. Serrano, and S. So. 2009. "Differential Gene Expression in the Perichondrium and Cartilage of the Neonatal Mouse Temporomandibular Joint." *Orthod Craniofac Res.* 12(3):168–77.

Johnstone, Brian et al. 2012. "Tissue Engineering for Articular Cartilage Repair - The State of the Art." *European Cells and Materials* 25:248–67.

Jullien, Nicolas. n.d. "AmplifX."

Kaiser, Meghann L. et al. 2006. "Cartilage Regeneration in the Rabbit Nasal Septum." *Laryngoscope*

116(10):1730–34.
Lee, Juliana Tsz Yan, Kenneth Man Chi Cheung, and Victor Yu Leong Leung. 2015. "Extraction of RNA from Tough Tissues with High Proteoglycan Content by Cryosection, Second Phase Separation and High Salt Precipitation." *Journal of Biological Methods* 2(2):20.
Liu, Yu, Guangdong Zhou, and Yilin Cao. 2017. "Recent Progress in Cartilage Tissue Engineering—Our Experience and Future Directions." *Engineering* 3(1):28–35.
Mobasheri, Ali et al. 2018. "The Chondrocyte Channelome: A Narrative Review." *Joint Bone Spine* (2017):1–7.
Muir, Helen. 1995. "The Chondrocyte, Architect of Cartilage. Biomechanics, Structure, Function and Molecular Biology of Cartilage Matrix Macromolecules." *BioEssays* 17(12):1039–48.
Mumme, Marcus, Andrea Barbero, et al. 2016. "Nasal Chondrocyte-Based Engineered Autologous Cartilage Tissue for Repair of Articular Cartilage Defects: An Observational First-in-Human Trial." *The Lancet* 388(10055):1985–94.
Mumme, Marcus, Amir Steinitz, et al. 2016. "Regenerative Potential of Tissue-Engineered Nasal Chondrocytes in Goat Articular Cartilage Defects." *Tissue Engineering Part A* 22(21–22):1286–95.
Music, E., K. Futrega, and M. R. Doran. 2018. "Sheep as a Model for Evaluating Mesenchymal Stem/Stromal Cell (MSC)-Based Chondral Defect Repair." *Osteoarthritis and Cartilage* 26(6):730–40.
Nathaniel, P., Van C. Mow, and Robert J. Foster. 1998. "Composition and Dynamics of Articular Cartilage: Structure, Function, and Maintaining Healthy State." *Journal of Orthopaedic & Sports Physical Therapy* 28:203–15.
Pelttari, Karoliina et al. 2014. "Adult Human Neural Crest-Derived Cells for Articular Cartilage Repair." *Science Translational Medicine* 6(251).
Pelttari, Karoliina, Anke Wixmerten, and Ivan Martin. 2009. "Do We Really Need Cartilage Tissue Engineering?" *Swiss medical weekly : official journal of the Swiss Society of Infectious Diseases, the Swiss Society of Internal Medicine, the Swiss Society of Pneumology* 139(41–42):602–9.
Pollard, Thomas D., William C. Earnshaw, Jennifer Lippincott-Schwartz, and Graham T. Johnson. 2017. *Cell Biology*. 3rd ed. Elsevier.
Popko, Mariola, Ronald L. A. W. Bleys, Jan-Willem De Groot, and Egbert H. Huizing. 2007. "Histological Structure of the Nasal Cartilages and Their Perichondrial Envelope I. The Septal and Lobular Cartilage." *Rhinology* 45:148–52.
Ross, Michael H. and Wojciech Pawlina. 2010. *Histology: A Text and Atlas with Correlated Cell and Molecular Biology*. 6th ed. LWW.
Rotter, Nicole et al. 2002. "Age Dependence of Biochemical and Biomechanical Properties of Tissue-Engineered Human Septal Cartilage." *Biomaterials* 23(15):3087–94.
Sharifi, Ali Mohammad, Ali Moshiri, and Ahmad Oryan. 2016. "Articular Cartilage: Injury, Healing, and Regeneration."
Skoog, Tord, Lennart Ohlséan, and Stephen A. Sohn. 1972. "Perichondrial Potential for Cartilagenous Regeneration." *Scandinavian Journal of Plastic and Reconstructive Surgery and Hand Surgery* 6(2):123–25.
Späth, Stephan-Stanislaw, Anenisia C. Andrade, Michael Chau, Marta Baroncelli, and Ola Nilsson. 2018. "Evidence That Rat Chondrocytes Can Differentiate Into Perichondrial Cells." *JBMR Plus* 2(6):351–61.
Tae Kyun, Kim. 2015. "T Test as a Parametric Statistic." *Korean Journal of Anesthesiology* 68(6):540–46.
Treilleux, Isabelle, Frederic Mallein-Gerin, Dominique Le Guellec, and Daniel Herbage. 1992. "Localization of the Expression of Type I, II, III Collagen, and Aggrecan Core Protein Genes in Developing Human Articular Cartilage." *Matrix* 12(3):221–32.
Verwoerd-Verhoef, Henriette L., Paul G. J. Ten Koppel, Gerjo J. V. M. Van Osch, Cees A. Meeuwis, and Carel D. A. Verwoerd. 1998. "Wound Healing of Cartilage Structures in the Head and Neck Region." *International Journal of Pediatric Otorhinolaryngology* 43(3):241–51.
Vinatier, C. and J. Guicheux. 2016. "Cartilage Tissue Engineering: From Biomaterials and Stem Cells to Osteoarthritis Treatments." *Annals of Physical and Rehabilitation Medicine* 59(3):139–44.
Zaucke, Frank. 2016. "Cartilage Glycoproteins." Pp. 1–267 in *Cartilage: Volume 1: Physiology and Development*, vol. 1, edited by S. Grässel and A. Aszódi. Springer.

CURRICULUM VITAE

MATEA BREZAK

- 10000 Zagreb, Croatia

EDUCATION

2016 – 2019: Master of Molecular Biology
University of Zagreb, Faculty of Science - Molecular Biology, Zagreb (Croatia)

2013 – 2016: Bachelor of Science in Biology
University of Zagreb, Faculty of Science - Biology, Zagreb (Croatia)
bachelor thesis: „Genetics of Colon Cancer“; Dr Petra Korać, Assoc. Prof.

WORK EXPERIENCE

Apr 2018 – Feb 2019: Master student
University of Zagreb, Faculty of Science - Molecular Biology, Laboratory of Biomedicine; Dr Inga Marijanović, Assoc. Prof.
master thesis: „Characterization of newly-formed tissue after nasal septum cartilage biopsy “; Dr Inga Marijanović, Assoc. Prof., Maja Pušić, mag.biol.exp

Nov 2018 – Dec 2018: Demonstrator in Stem Cell Biology
University of Zagreb, Faculty of Science - Molecular Biology, Zagreb (Croatia)

PROJECTS

Apr 2015 – Noć biologije (GMOs: Pros and Cons)
Apr 2014 – Noć biologije (Nervous System Physiology)

CONFERENCES

Jun 2017 – Third Symposium of Life Sciences' Students
Nov 2016 – HDIR-4: "From Bench to Clinic„
-The 4TH Meeting with International Participation
Nov 2015 - HDBUZ: "1st Croatian Symposium of Biologists in Health Care"

LANGUAGES

Croatian – native speaker
English – C2
Italian – A1